Iranian Journal of Numerical Analysis and Optimization
Vol. 16, No. 3, 2026, pp 952–990
https://doi.org/10.22067/ijnao.2026.96513.1777
https://ijnao.um.ac.ir/

Research Article

A new numerical computational method for solving nonhomogeneous time-fractional nonlinear parabolic problems in unbounded domains

S.A. Ghanizadeh and M.H. Akrami*,

Abstract

This paper addresses the numerical solution of nonhomogeneous time-fractional nonlinear parabolic problems defined on unbounded domains, where challenges arise due to temporal nonlocality, nonlinear dynamics, and the infinite spatial extent. To overcome these difficulties, we propose a novel computational framework that transforms the original unbounded domain problem into an equivalent formulation on a bounded domain through the construction of absorbing boundary conditions. Unlike existing approaches that rely on Padé approximations, our method directly utilizes the fundamental properties of fractional derivatives to define these boundaries more accurately. The resulting problem is then discretized using a high-order finite difference scheme, allowing for efficient and precise numerical implementation. Theoretical analysis confirms that the method is stable and ensures controlled computational error. Numerical experiments demonstrate the practical effectiveness of the proposed approach, achieving accurate results with significantly reduced computational cost. This method provides a reliable

*Corresponding author

Received 15 November 2025; revised 5 January 2026; accepted 19 May 2026

Mohammad Hossein Akrami,
Associate Professor, Department of Applied Mathematics, Faculty of Science, Yazd University, Yazd, Iran. e-mail: akrami@yazd.ac.ir

Seyed Ali Ghanizadeh
Department of Applied Mathematics, Faculty of Science, Yazd University, Yazd, Iran. e-mail: ghanizadeh@stu.yazd.ac.ir

How to cite this article
Ghanizadeh, S.A. and Akrami, M.H., A new numerical computational method for solving nonhomogeneous time-fractional nonlinear parabolic problems in unbounded domains. *Iran. J. Numer. Anal. Optim.*, 2026; 16(3): 952-990. https://doi.org/10.22067/ijnao.2026.96513.1777

and efficient tool for modeling diffusion phenomena governed by time-fractional dynamics in unbounded spatial settings.

AMS subject classifications (2020): Primary 35R11, 65M06; Secondary 35K55, 65M12, 65N06.

Keywords: Absorbing boundary conditions; High-order finite difference; Nonlinear parabolic equations.

1 Introduction

Over the past several decades, fractional partial differential equations (FPDEs) have gained significant attention in mathematical research owing to their exceptional ability to model complex physical systems exhibiting memory and hereditary properties [2, 6, 10, 17, 22]. These equations have found extensive applications in diverse scientific disciplines, including biology, chemistry, and various other fields that can be described through mathematical frameworks. FPDEs have become particularly valuable for representing anomalous diffusion processes and nonlocal phenomena. A fundamental characteristic of these equations involves the replacement of the conventional first-order time derivative in standard diffusion equations with a fractional-order derivative of degree α, where the parameter α satisfies $0 < \alpha < 2$. The resulting equations exhibit distinct behaviors depending on the fractional order for $0 < \alpha < 1$, the system demonstrates sub-diffusive properties while values in the range $1 < \alpha < 2$ correspond to fractional wave dynamics. Recent years have witnessed substantial progress in both theoretical analysis and numerical approximation techniques for FPDEs. Nevertheless, obtaining closed-form analytical solutions remains challenging in most practical cases, and often proves intractable due to the inherent complexity of these fractional-order systems [5, 12, 15, 18]. Even when analytical solutions to fractional differential equations are attainable in specialized cases, they frequently incorporate sophisticated special functions such as Fox-H, Wright, and Mittag-Leffler functions. The numerical computation of these functions presents significant computational difficulties due to their inherent complexity. The increasing necessity for practical implementations in engineering and applied sciences has consequently stimulated substantial progress in developing robust numerical approaches for solving FPDEs. Among these, finite difference methods have emerged as particularly important for approximating solutions to time-fractional differential equations. Previous investigations have predominantly concentrated on initial-boundary value problems defined over finite spatial domains. As a representative example, Zhuang and Liu [5] examined one-dimensional sub-diffusion equations with Caputo time-fractional derivatives, introducing a numerical scheme that employs the $L1$ approximation for the Caputo derivative. Their work rigorously established the stability and convergence properties of this method [5, 27]. It is in related developments that Murillo and Yuste presented explicit finite difference schemes and carried out detailed stability analyses by numerical experimentation. Alternatively, Sun and Wu [5] developed their numerical scheme based on implicit discretization, where a full theoretical justification was given using discrete energy methods [5, 23]. A significant volume of research effort has been devoted to problems posed on unbounded spatial domains since such problems are of crucial importance in the mathematical modeling of heat conduction in solids, fluid flow, as well as problems arising from financial mathematics, for example, option pricing theory [5, 8, 9]. Fractional equations in unbounded domains were first studied in the 1980s. For instance, Weiss and co-authors mainly researched the analysis and the derivation of the analytic solution to fractional diffusion equations; typically, the solutions were expressed with complex functions like Fox-H functions [5, 21, 26]. However, numerical research in this area is still in its infancy, with only a few scattered studies addressing this topic [1, 5, 6, 16, 19, 20]. One of the effective numerical schemes for such a class of differential equations involves the use of absorbing boundary conditions (ABCs). In general, time-FPDEs defined on unbounded (infinite) domains are computationally demanding, as they require complex and intensive computation for very large spatial intervals. An ABC essentially transforms a problem that is initially defined on an unbounded spatial domain ($\chi \in \mathbb{R}$) into a boundary value problem on a bounded domain. This not only reduces the computational complexity but also helps preserve the solution's essential features. A number of studies on the design of ABCs for fractional equations have been carried out. Some of them are given below:

- Gao, Sun, and Zhang [5] consider fractional-time diffusion equations in unbounded spatial domains. They first derived accurate artificial boundary conditions using the Laplace transform and then transferred the problem to a bounded domain and proposed a stable and convergent finite difference scheme with accuracy $O(\varrho^{2-\alpha} + h^2)$, where ϱ and h are time and space step size, respectively. For the compact case, they also developed and presented a numerical method with higher accuracy, $O(\varrho^{2-\alpha} + h^4)$.

- Gao and Sun [6] used the Laplace transform to derive accurate artificial boundary conditions and employing the method of order reduction. Then, they transformed the fractional-time differential equations problem in an infinite domain into a solvable model in a bounded domain and solved it.

- Li and Zhang [14] proposed a numerical method for solving nonlinear fractional-time equations in unbounded domains, where the exact ABCs are derived using the Laplace transform. Additionally, to simplify the nonlinear part, they used a Padé approximation for the linearized finite difference scheme, eliminating the need for iterative methods to solve the problem.

Now, based on the aforementioned papers and the explanations provided regarding the background of such problems, in this paper, we consider the following nonhomogeneous problem:

$$\begin{cases} {}_0^C D_\rho^\alpha \xi(\chi,\rho) = \xi_{\chi\chi}(\chi,\rho) + \mathcal{F}(\xi(\chi,\rho)) + \mathcal{G}(\chi,\rho) \quad \chi \in \mathbb{R}, \quad 0 < \rho \le P, \\ \xi(\chi,0) = \xi_0(\chi), \quad (\chi,\rho) \in \mathbb{R}, \\ \xi(\chi,\rho) \to 0, \quad |\chi| \to \infty, \end{cases} \tag{1}$$

where the initial function $\xi_0(\chi)$ has compact support, meaning that it is nonzero only within a finite interval, and is exactly zero outside this interval. Here, $\xi(\chi,\rho)$ is the unknown real-valued solution of the problem. The operator ${}_0^C D_\rho^\alpha$ denotes the Caputo fractional derivative of order α, which is defined for sufficiently smooth functions $\xi(\chi,\rho) \in C^n[0,P]$ by

$$\begin{aligned} {}_0^C D_\rho^\alpha\, \xi(\chi,\rho) = \frac{1}{\Gamma(n-\alpha)} \int_0^\rho \frac{\partial^n \xi(\chi,\vartheta)}{\partial \vartheta^n} \frac{1}{(\rho-\vartheta)^{\alpha-n+1}}\, d\vartheta, \\ n-1 < \alpha < n,\ n \in \mathbb{N}, \end{aligned} \tag{2}$$

where $\Gamma(\cdot)$ denotes the Gamma function. In particular, for the case $0 < \alpha < 1$, we obtain

$${}_0^C D_\rho^\alpha\, \xi(\chi,\rho) = \frac{1}{\Gamma(1-\alpha)} \int_0^\rho \frac{\partial \xi(\chi,\vartheta)}{\partial \vartheta} \frac{1}{(\rho-\vartheta)^{\alpha}}\, d\vartheta. \tag{3}$$

Throughout this work, we mainly focus on the case $0 < \alpha < 1$, and therefore the simplified form (3) will be used [12, 18]. The nonlinear term $\mathcal{F}(\xi)$ and the term $\mathcal{G}(\chi,\rho)$ appear in different forms for various problems. This equation is well-suited for modeling anomalous diffusion processes and complex systems where memory effects and nonlocal temporal behaviors play an important role. Such equations are frequently used in scientific and engineering fields to describe phenomena with long-term memory or systems with history-dependent behaviors. In this work, we convert the original unbounded domain problem into an equivalent bounded domain formulation by developing ABCs. Unlike traditional methods based on Padé approximations, our approach directly applies the inherent properties of fractional derivatives to define these boundaries with improved accuracy. The reformulated problem is then discretized using a high-order finite difference scheme, enabling efficient and precise numerical solutions. In recent years, Caputo fractional derivatives have attracted significant attention due to their ability to accurately model memory-dependent processes in various physical and engineering applications. Several recent studies have focused on the analytical and numerical treatment of fractional differential equations involving Caputo operators, highlighting their effectiveness in capturing anomalous diffusion phenomena. For instance, the works reported in [24, 25] investigate advanced numerical schemes and theoretical properties of Caputo-type fractional models, providing important insights into stability, convergence, and computational efficiency. These developments further motivate the present investigation on high-order numerical methods for time-fractional nonlinear parabolic equations.

2 Problem formulation

Solving partial differential equations (PDEs) on unbounded domains directly presents significant challenges. A common technique to address these challenges involves employing ABCs. The main objective of the ABCs is to simulate the behavior of infinite boundaries by adding special conditions at the boundaries of a finite domain. These boundary conditions act in such a way that waves or information approaching the boundaries of the finite domain are absorbed, preventing their reflection back into the domain [4]. In fact, incoming waves smoothly dissipate at the boundary without causing disruption or reflection within the domain. In this way, the numerical solution of the problem on a finite domain closely approximates the real solution on an infinite domain. For example, if a fractional-time differential problem is defined on an infinite domain ($\chi \in \mathbb{R}$), then the domain is reduced to a finite interval $[a, b]$ for numerical solution. The use of ABCs at the points $\chi = a$ and $\chi = b$ ensures that the value of the function near the boundaries naturally tends to zero. Thus, the ABCs conditions are designed in such a way that they simulate the behavior $\lim_{|\chi|\to\infty} \xi(\chi, \rho) = 0$ at the artificial boundaries. In practice, the Laplace transform provides a powerful analytical tool for constructing accurate ABCs in problems defined on unbounded spatial domains. Direct numerical computation over an infinite region is generally infeasible. Therefore, it is essential to reformulate the problem on a finite computational interval while preserving the physical behavior at infinity. By applying the Laplace transform to the governing equation, one can analytically derive exact boundary conditions that emulate the decay of the solution at infinity. This procedure effectively eliminates artificial wave reflections from the truncated boundaries and ensures that the numerical solution within the bounded region accurately represents the true dynamics of the original unbounded problem. Without implementing accurate ABCs, performing numerical simulations over unbounded domains becomes either impractical or leads to results contaminated by large errors and high computational costs. Hence, the application of the Laplace transform in constructing exact ABCs is essential. Otherwise, one must either accept inaccurate numerical approximations or incur prohibitively high computational expenses both of which are far from ideal for reliable numerical modeling. It is important to note that the nonlinear term is restricted to the interior computational domain, while the exterior region is assumed to be linear. Under this assumption, the ABCs derived through the Laplace transform remain mathematically valid and physically consistent. In this study, taking into account that the solution $\xi(\chi,\rho)$ vanishes as $|\chi| \to \infty$, a direct relationship between its spatial derivative and the fractional time derivative of order $(\frac{\alpha}{2})$ is derived. This relation serves as the exact ABC, ensuring that the outgoing energy and information approaching the boundaries are naturally absorbed instead of being reflected back into the computational domain. Consequently, artificial reflections are effectively eliminated, leading to a substantial improvement in the accuracy and stability of the numerical solution. In this study, our focus is on the fractional-time diffusion equation in an infinite spatial domain, as shown in (1). First, we consider two artificial boundary points for the left and right sides of the domain as follows:

$$\begin{cases} \Lambda_- := \{\chi | \chi = I_-\}, \\ \Lambda_+ := \{\chi | \chi = I_+\}. \end{cases}$$

Then, we divide the entire domain $\mathbb{R}$ into three sections:

$$\begin{cases} \mathit{\Delta}_- := \{\chi \mid -\infty < \chi < I_-\}, \\ \mathit{\Delta}_i := \{\chi \mid I_- \leq \chi \leq I_+\}, \\ \mathit{\Delta}_+ := \{\chi \mid I_+ < \chi < +\infty\}. \end{cases} \tag{4}$$

The exterior of the domain is denoted by $\mathit{\Delta}_e = \mathit{\Delta}_- \cup \mathit{\Delta}_+$. The constants I_- and I_+ are chosen such that the initial function $\xi_0(\chi)$ takes nonzero values only within the interior region of the domain $\mathit{\Delta}_i$ and is exactly zero outside of it. The form of the operator equation (1) in $\mathit{\Delta}_e$ is written as follows:

$$ {}_0^C D_\rho^\alpha \xi(\chi,\rho) = \mathcal{L}\xi(\chi,\rho) + \mathcal{N}\xi(\chi,\rho), \quad \chi \in \mathit{\Delta}_e, \tag{5}$$

where

$$\mathcal{L}\xi = \xi_{\chi\chi}, \qquad \mathcal{N}\xi = \mathcal{F}(\xi) + \mathcal{G}(\chi,\rho).$$

Considering the linear part of (5), we have

$$ {}_0^C D_\rho^\alpha \xi(\chi,\rho) = \xi_{\chi\chi}(\chi,\rho). \tag{6}$$

The Laplace transform of the Caputo fractional derivative for $0 < \alpha < 1$ is given by [18]:

$$\begin{aligned}\mathcal{L}[{}^C_0D^{\alpha}_{\rho}\xi(\chi,\rho)](\vartheta) =& \vartheta^{\alpha}\mathcal{L}[\xi(\chi,\rho)](\vartheta) - \vartheta^{\alpha-1}\xi(\chi,0)\\ =& \vartheta^{\alpha}\tilde{\xi}(\chi,\vartheta) - \vartheta^{\alpha-1}\xi(\chi,0).\end{aligned} \tag{7}$$

Thus, we first restrict the problem (1) to the domain $\varDelta_e$, where $\mathcal{F}(\xi(\chi,\rho)) \approx 0$ and $\mathcal{G}(\chi,\rho) \approx 0$. Now, considering the initial condition $\xi_0(\chi) = 0$ for $\chi \in \varDelta_e$, (6) can be rewritten in the Laplace space as follows:

$$\vartheta^{\alpha}\tilde{\xi}(\chi,\vartheta) = \tilde{\xi}_{\chi\chi}(\chi,\vartheta), \quad \mathrm{Re}(\vartheta) > 0. \tag{8}$$

Equation (8) has a general solution given as follows:

$$\tilde{\xi}(\chi,\vartheta) = \mathcal{A}_1(\vartheta)e^{-\sqrt{\vartheta^{\alpha}}\chi} + \mathcal{A}_2(\vartheta)e^{\sqrt{\vartheta^{\alpha}}\chi}, \tag{9}$$

where $\mathcal{A}_1(\vartheta)$ and $\mathcal{A}_2(\vartheta)$are unknown parameters. Given that $\xi(\chi,\vartheta) \to 0$ as $|\chi| \to \infty$, we have

$$\tilde{\xi}(\chi,\vartheta) = \begin{cases} \mathcal{A}_1(\vartheta)e^{-\sqrt{\vartheta^{\alpha}}\chi}, & \chi \in \varDelta_+,\\ \mathcal{A}_2(\vartheta)e^{\sqrt{\vartheta^{\alpha}}\chi}, & \chi \in \varDelta_-.\end{cases} \tag{10}$$

Differentiating $\tilde{\xi}(\chi,\vartheta)$ with respect to χ, yields

$$\frac{\partial\tilde{\xi}(\chi,\vartheta)}{\partial\chi} = \begin{cases} -\sqrt{\vartheta^{\alpha}}\,\tilde{\xi}(\chi,\vartheta) = -\vartheta^{\frac{\alpha}{2}}\tilde{\xi}(\chi,\vartheta), & \chi \in \varDelta_+,\\ \sqrt{\vartheta^{\alpha}}\,\tilde{\xi}(\chi,\vartheta) = \vartheta^{\frac{\alpha}{2}}\tilde{\xi}(\chi,\vartheta), & \chi \in \varDelta_-.\end{cases} \tag{11}$$

Now, applying the inverse Laplace transform to (11), implies

$$\frac{\partial\xi(\chi,\rho)}{\partial\chi} = \begin{cases} -\frac{1}{\Gamma(1-\frac{\alpha}{2})}\int_0^{\rho}(\rho-\vartheta)^{-\frac{\alpha}{2}}\frac{\partial\xi(\chi,\vartheta)}{\partial\vartheta}\,d\vartheta = -{}^C_0D^{\frac{\alpha}{2}}_{\rho}\xi(\chi,\rho), & \chi \in \varDelta_+,\\ \frac{1}{\Gamma(1-\frac{\alpha}{2})}\int_0^{\rho}(\rho-\vartheta)^{-\frac{\alpha}{2}}\frac{\partial\xi(\chi,\vartheta)}{\partial\vartheta}\,d\vartheta = {}^C_0D^{\frac{\alpha}{2}}_{\rho}\xi(\chi,\rho), & \chi \in \varDelta_-.\end{cases} \tag{12}$$

By taking the limit as $\chi \to I_+$ and $\chi \to I_-$, and assuming the smoothness of $\xi(\chi,\rho)$ at $\chi = I_-$ and $\chi = I_+$, we obtain the following relation:

$$\begin{cases} \frac{\partial\xi(I_+,\rho)}{\partial\chi} = -{}^C_0D^{\frac{\alpha}{2}}_{\rho}\xi(I_+,\rho),\\ \frac{\partial\xi(I_-,\rho)}{\partial\chi} = {}^C_0D^{\frac{\alpha}{2}}_{\rho}\xi(I_-,\rho).\end{cases} \tag{13}$$

In this work, the interrelation between the Caputo and Riemann–Liouville fractional derivatives is implicitly exploited in the analytical formulation of the ABCs. Specifically, since the function $\xi(\chi,\rho)$ is defined such that all its integer-order time derivatives vanish at the initial point ($\rho = 0$), the Caputo and Riemann–Liouville derivatives become equivalent in this setting. Under this assumption, the composition property of the Riemann–Liouville derivative can be consistently extended to the Caputo derivative. Consequently, the following relation holds and is analytically justified based on the fundamental properties of fractional calculus:

$$ {}_0^C D_\rho^{\frac{\alpha}{2}} \left({}_0^C D_\rho^{\frac{\alpha}{2}} \xi(\chi,\rho) \right) = {}_0^C D_\rho^{\alpha} \xi(\chi,\rho). $$

Now, applying the fractional derivative ${}_0^C D_\rho^{\frac{\alpha}{2}}$ to relation (13), gives

$$ \begin{cases} {}_0^C D_\rho^{\alpha} \xi(\chi,\rho) = -{}_0^C D_\rho^{\frac{\alpha}{2}} \xi_\chi(\chi,\rho) & \chi = I_+, \\ {}_0^C D_\rho^{\alpha} \xi(\chi,\rho) = {}_0^C D_\rho^{\frac{\alpha}{2}} \xi_\chi(\chi,\rho) & \chi = I_-. \end{cases} \tag{14} $$

At this stage, the exact artificial boundary conditions (14) for the problem (1) have been obtained. Considering (14), we observe that these boundary conditions involve fractional time derivatives of order $\frac{\alpha}{2}$, which is half of the time derivative order in the governing equation (1). Thus, the original problem (1) is reduced to an IVP problem in the bounded domain Δ_i and can be written as follows:

$$ \begin{aligned} &{}_0^C D_\rho^{\alpha} \xi(\chi,\rho) = \xi_{\chi\chi}(\chi,\rho) + \mathcal{F}(\xi(\chi,\rho)) + \mathcal{G}(\chi,\rho), \quad (\chi,\rho) \in \Delta_i \times (0,P], \\ &{}_0^C D_\rho^{\frac{\alpha}{2}} \frac{\partial \xi(I_-,\rho)}{\partial \chi} = \xi_{\chi\chi}(I_-,\rho) + \mathcal{F}(\xi(I_-,\rho)) + \mathcal{G}(I_-,\rho), \quad \rho \in (0,P], \\ &{}_0^C D_\rho^{\frac{\alpha}{2}} \frac{\partial \xi(I_+,\rho)}{\partial \chi} = -(\xi_{\chi\chi}(I_+,\rho) + \mathcal{F}(\xi(I_+,\rho)) + \mathcal{G}(I_+,\rho)), \quad \rho \in (0,P], \\ &u(\chi,0) = \varphi(\chi), \qquad \chi \in \Delta_i = [I_-, I_+], \\ &u(0,\rho) = \phi(\rho), \qquad \rho \in (0,P]. \end{aligned} \tag{15} $$

Now, we transformed PDE with unbounded domain (1) into an equivalent bounded domain formulation by developing ABCs (15). This reformulation enables the solution of the modified problem, governed by (15), using an appropriate numerical methodology. In (15), the functions $\varphi(\chi)$ and $\phi(\rho)$ are known functions determined by the given source term and initial data of the original problem (1), and they arise naturally from the reformulation of the nonhomogeneous term after imposing the ABCs.

3 Numerical technique

This section presents a novel numerical methodology for solving the boundary-value problem governed by (15). It is organized into three main components:

(1) the derivation of a high-order approximation scheme for fractional derivatives,
(2) the development of an efficient high-order finite difference framework based on this approximation, and
(3) the implementation of the proposed numerical scheme to solve the considered problem.

Compared with classical time discretization methods for Caputo fractional derivatives, such as the $L1$ scheme with accuracy $\mathcal{O}(\varrho^{2-\alpha})$, the proposed high-order finite difference approximation achieves a temporal accuracy of $\mathcal{O}(\varrho^{3-\alpha})$. This improvement significantly reduces the numerical error for long-time simulations and allows the use of relatively larger time step sizes without sacrificing accuracy. Moreover, the higher-order approximation enhances the stability properties of the numerical scheme, particularly in the presence of ABCs involving fractional derivatives of order $\alpha/2$. As a result, the proposed method provides a more accurate and efficient computational framework compared with standard low-order schemes, especially for nonlinear fractional diffusion problems posed on unbounded spatial domains.

3.1 Approximation of fractional derivative

This part establishes high-order numerical approximations for the Caputo fractional derivative. The accuracy of this method depends on the parameter $\alpha \in (0,1)$. First, we introduce a $(3-\alpha)$-order approximation, which was proposed in [13]. For simplification, in this subsection, we consider one variable function $\xi(\rho)$, and suppose that $\xi(\rho) \in C^6[0,P]$, that $\xi^{(5)}(\rho)$ is continuous, and that $\xi^{(6)}(\rho)$ exists in the interval $[0,P]$. Additionally, $0 = \rho_0 < \rho_1 < \ldots < \rho_N = P$ is given for a positive integer $N > 0$, where $\rho_k = k\varrho$, $k = 0,1,\ldots,N$, and $\varrho = \frac{P}{N}$ is the time step size. First, we write the Taylor expansion of the function $\xi'(\vartheta)$ around the point $\rho = \rho_j$, where $0 \le j < k$. We have

$$\begin{aligned}\xi^{'}(\vartheta) =& \xi^{'}(\rho_j) + \xi^{''}(\rho_j)(\vartheta-\rho_j) + \frac{\xi^{'''}(\rho_j)}{2!}(\vartheta-\rho_j)^2 \\ &+ O((\vartheta-\rho_j)^3), \qquad \vartheta \in (\rho_j, \rho_{j+1}).\end{aligned} \tag{16}$$

This expansion shows that the first derivative of the function at the point ϑ is computed as a linear combination of higher-order derivatives at the point ρ_j. Now, consider the following relations for the first and second derivatives:

$$\xi^{'}(\rho_j) = \frac{\xi(\rho_{j+1}) - \xi(\rho_{j-1})}{2\varrho} - \frac{\xi^3(\rho_j)}{3!}\varrho^2 + O(\varrho^4), \tag{17}$$

and

$$\xi^{''}(\rho_j) = \frac{\xi(\rho_{j+1}) - 2\xi(\rho_j) + \xi(\rho_{j-1})}{\varrho^2} - \frac{\xi^4(\rho_j)}{12}\varrho^2 + O(\varrho^4). \tag{18}$$

By substituting (17) and (18) into (16), we arrive at the following relation:

$$\begin{aligned}\xi^{'}(\vartheta) =& \frac{\xi(\rho_{j+1}) - \xi(\rho_{j-1})}{2\varrho} + \frac{\xi(\rho_{j+1}) - 2\xi(\rho_j) + \xi(\rho_{j-1})}{\varrho^2}(\vartheta - \rho_j) - \frac{\xi^3(\rho_j)}{3!}\varrho^2 \\ &+ \frac{\xi^3(\rho_j)}{2!}(\vartheta - \rho_j)^2 + O((\vartheta - \rho_j)^3), \quad 0 < \vartheta - \rho_j < \varrho. \end{aligned} \tag{19}$$

This approximate relation defines the derivative $\xi'(\rho)$ by considering the integrals corresponding to the third-order derivatives over the specified interval. By applying relation (19), the Caputo derivative approximation with the condition ($0 < \alpha < 1$) is written as follows:

$$\begin{aligned}{}^C_0D^\alpha_\rho \xi(\rho)|_{\rho=\rho_k} =& \frac{1}{\Gamma(1-\alpha)}\int_0^{\rho_k}(\rho_k - \vartheta)^{-\alpha}\xi^{'}(\vartheta)d\vartheta \\ =& \frac{1}{\Gamma(1-\alpha)}\sum_{j=0}^{k-1}\int_{\rho_j}^{\rho_{j+1}}(\rho_k - \vartheta)^{-\alpha}\xi^{'}(\vartheta)d\vartheta \\ =& \frac{1}{\Gamma(1-\alpha)}\sum_{j=0}^{k-1}\int_{\rho_j}^{\rho_{j+1}}(\rho_k - \vartheta)^{-\alpha}(\frac{\xi(\rho_{j+1}) - \xi(\rho_{j-1})}{2\varrho} \\ &+ \frac{\xi(\rho_{j+1}) - 2\xi(\rho_j) + \xi(\rho_{j-1})}{\varrho^2}(\vartheta - \rho_j) - \frac{\xi^3(\rho_j)}{3!}\varrho^2 \\ &+ \frac{\xi^3(\rho_j)}{2!}(\vartheta - \rho_j)^2)d\vartheta + O((\vartheta - \rho_j)^3) \\ =& \frac{\varrho^{-\alpha}}{\Gamma(3-\alpha)}\sum_{j=0}^{k-1}(\omega_{1,k-j}(\xi^{j+1} - \xi^{j-1}) \\ &+ \omega_{2,k-j}(\xi^{j+1} - 2\xi^j + \xi^{j-1})) + \mathcal{R}^k, \end{aligned} \tag{20}$$

where $\mathcal{R}^k \leq C\varrho^{3-\alpha}$ [13]. Relation (20) represents the Caputo fractional-time derivative applied to solve the problem in (1). Following the approximation framework established in [3, Lemma 2.1], weighting coefficients defined in (20) are derived as follows:

$$\begin{cases} \omega_{1,n} = \frac{2-\alpha}{2}\left((n)^{1-\alpha} - (n-1)^{1-\alpha}\right), \\ \omega_{2,n} = (n)^{2-\alpha} - (n-1)^{2-\alpha} - (2-\alpha)(n-1)^{1-\alpha}. \end{cases} \tag{21}$$

Therefore, fractional-time derivative of relation (20) is written as follows:

$$
\begin{aligned}
{}_0^C D_\rho^\alpha \xi(\rho)|_{\rho=\rho_k} =& \frac{\varrho^{-\alpha}}{\Gamma(3-\alpha)} \sum_{j=0}^{k-1} (\omega_{1,k-j}(\xi^{j+1}-\xi^{j-1}) \\
&+ \omega_{2,k-j}(\xi^{j+1}-2\xi^{j}+\xi^{j-1})) + O(\varrho^{3-\alpha}). \qquad (22)
\end{aligned}
$$

In formula (22), if $j=0$, then the value $\xi^{j-1}=\xi^{-1}$ is defined outside the interval $[0,P]$. Here, several choices are presented for approximating ξ^{-1} . In numerical computations, values of the neighboring function are mainly used to approximate ξ^{-1} such that

$$
\xi^{-1} = \xi(0) - \varrho\xi'(0) + \frac{\varrho^2}{2}\xi''(0) + O(\varrho^3).
$$

1. When $\xi'(0)=0$ and $\xi''(0)=0$, we have $\xi^{-1}=\xi^0+O(\varrho^3)$, where the convergence order of formula (22) is $O(\varrho^{3-\alpha})$.

2. When $\xi'(0)=0$ and $\xi''(0)\neq 0$, we have $\xi^{-1}=\xi^0+\frac{\varrho^2}{2}\xi''(0)+O(\varrho^3)$. In this case, the convergence order of formula (22) is $O(\varrho^2)$.

3. When $\xi'(0)\neq 0$, the convergence order is $O(\varrho)$.

Lemma 1. [7] The coefficients $\omega_{1,k-j}$ and $\omega_{2,k-j}$ in relation (22) have the following properties:

(I) Initial values of the coefficients:

$$
\omega_{1,1} = \frac{2-\alpha}{2}, \quad \omega_{2,1} = 1.
$$

Assume that $0<\alpha<1$.

(II) Constraints and behavior of the coefficients:

$$
\begin{cases}
0 < \omega_{1,r-j+1} < \omega_{1,r-j} \leq \frac{2-\alpha}{2} < 1, \\
0 < \omega_{2,r-j+1} < \omega_{2,r-j} \leq 1.
\end{cases}
$$

(III) Difference between adjacent coefficients:

$$
\begin{cases}
\omega_{1,r-j+1} - \omega_{1,r-j} > \omega_{1,r-j} - \omega_{1;r-j-1}, & r-j \geq 2, \\
\omega_{2,r-j+1} - \omega_{2,r-j} > \omega_{2,r-j} - \omega_{2,r-j-1}, & r-j \geq 2.
\end{cases}
$$

(IV) Sum of coefficients:

$$\omega_{1,2}+\omega_{1,1}+\omega_{2,2}-\omega_{2,1}\begin{cases}>0, & \alpha\in(0,\alpha_0),\\ \leq 0, & \alpha\in[\alpha_0,1),\end{cases}$$

which $\alpha_0 \approx 0.68$ is the root of the equation

$$(6-\alpha)2^{-\alpha}+\alpha-4=0,\quad \alpha\in(0,1),$$

and also,

$$\omega_{1,r-j}+\omega_{1,r-j-1}+\omega_{2,r-j}-\omega_{2,r-j-1}>0,\quad r-j\geq 3.$$

(V) Special combinations of the coefficients:

$$\begin{aligned}&-\omega_{1,2}+2\omega_{2,1}-\omega_{2,2}>0,\\ &\omega_{1,3}-\omega_{1,1}+\omega_{2,3}-2\omega_{2,2}+\omega_{2,1}\begin{cases}>0, & \alpha\in(0,\alpha_1),\\ \leq 0, & \alpha\in[\alpha_1,1),\end{cases}\end{aligned}$$

that $\alpha_1 \approx 0.37$ is the root of the equation

$$-2^{3-\alpha}+3\cdot 2^{2-\alpha}-2^{1-\alpha}+2^{-\alpha}-\frac{3(2-\alpha)^2}{2^{1-\alpha}}-3\alpha^2+6=0,\quad \alpha\in(0,1),$$

and also,

$$\omega_{1,r-j+1}-\omega_{1,r-j-1}+\omega_{2,r-j+1}-2\omega_{2,r-j}+\omega_{2,r-j-1}<0,\quad r-j\geq 3.$$

In this work, a high-order finite difference approximation with temporal accuracy of $O(3-\alpha)$ is adopted for discretizing the fractional-time derivative, as presented in (22). This scheme achieves higher accuracy than the classical $L1$ method, whose convergence order is $O(2-\alpha)$. The enhanced accuracy enables the method to produce reliable results even for relatively large time step sizes. Moreover, since the ABCs are analytically and exactly formulated, numerical disturbances due to wave reflections at the boundaries are effectively eliminated, which plays a crucial role in maintaining the stability of the proposed numerical scheme (28).

3.2 Construction of the finite difference method

Assume that $\varrho = \frac{P}{N}$ and $h = \frac{I_+ - I_-}{M}$ are the time and spatial step sizes, respectively, where M and N are given positive integers. The spacing between the grid points in the temporal and spatial dimensions is considered as follows:

$$\begin{cases} \chi_i = ih, \quad 0 \le i \le M, \\ \rho_k = k\varrho, \quad 0 \le k \le N, \end{cases}$$

and the computational domain is partitioned into two structured grids:

$$\Pi_\varrho = \{\rho_k \mid 0 = \rho_0 < \rho_1 < \cdots < \rho_N = P\},$$

$$\Pi_h = \{\chi_i \mid \chi_i = I_- + ih,\ 0 \le i \le M\}.$$

Assume that ξ_i^k is the numerical approximation of $\xi(\chi_i, \rho_k)$, we define the space of grid functions defined on $\Pi_\tau \times \Pi_h$ as follows:

$$\mathcal{V} = \{\xi_i^k \mid 0 \le i \le M,\ 0 \le k \le N\}.$$

To facilitate the subsequent numerical analysis, the following systematic notation is formally defined:

$$\begin{cases} \sigma_\chi \xi^k_{i-\frac{1}{2}} = \frac{\xi_i^k - \xi_{i-1}^k}{h}, \quad \sigma_\chi^2 \xi_i^k = \frac{\sigma_\chi \xi^k_{i+\frac{1}{2}} - \sigma_\chi \xi^k_{i-\frac{1}{2}}}{h}, \quad \mathcal{F}_v = \frac{\partial \mathcal{F}}{\partial \xi}\Big|_{\xi = v}, \\ \xi^k_{i+\frac{1}{2}} = \frac{1}{2}(\xi^k_{i+1} + \xi^k_i), \quad \sigma_\chi \xi^k_{i+\frac{1}{2}} = \frac{1}{h}(\xi^k_{i+1} - \xi^k_i). \end{cases}$$

For each $\xi, v \in \Pi_h$, the inner product and norm are expressed as

$$(\xi, v) = h \sum_{i=1}^{M} (\xi_{i-\frac{1}{2}} v_{i-\frac{1}{2}}),$$

$$\|\xi\| = \sqrt{(\xi,\xi)}, \quad \|\xi\|_1 = \sqrt{h \sum_{i=1}^{M} (\sigma_\chi \xi_{i-\frac{1}{2}})^2}, \quad \|\xi\|_\infty = \max_{0 \le i \le M} |\xi_i|.$$

The fractional-time derivative of relation (22) is rewritten as follows:

$$\begin{aligned} D_\varrho^\alpha \xi_i^k =& \mu_1 \sum_{j=0}^{k-1} (\omega_{1,k-i}(\xi_i^{j+1} - \xi_i^{j-1}) + \omega_{2,k-i}(\xi_i^{j+1} - 2\xi_i^j + \xi_i^{j-1})) \\ &+ O(\varrho^{3-\alpha}), \end{aligned} \tag{23}$$

where $\mu_1 = \frac{\varrho^{-\alpha}}{\Gamma(3-\alpha)}$. To address the computational complexity associated with the fractional differentiation of the nonlinear term $\mathcal{F}(\xi_i^k)$, the composition property of the Riemann–Liouville derivative together with its equivalence to the Caputo form is employed. This analytical manipulation enables the fractional derivative of order $(\frac{\alpha}{2})$ to act solely on $\mathcal{F}(\xi_i^k)$, while its influence is consistently controlled through the exact ABCs derived earlier. As a result, the nonlinear contribution is incorporated in a mathematically consistent and numerically stable manner within the proposed scheme.

In this paper, only one continuous mathematical model is investigated, namely the nonhomogeneous time-fractional nonlinear parabolic equation posed on an unbounded spatial domain, as introduced in (1). The formulation presented in (15) does not represent a new model; rather, it is an equivalent reformulation obtained by imposing exact ABCs on the original unbounded domain problem. The introduction of the auxiliary variable $v(\chi,\rho) = \xi_\chi(\chi,\rho)$ is carried out solely to facilitate the numerical discretization and the implementation of the ABCs involving fractional derivatives of order $\alpha/2$. This auxiliary reformulation does not alter the governing equation nor introduce additional modeling assumptions. Consequently, the continuous problems defined by (1) and (15) are mathematically equivalent, and the numerical scheme developed in section 3 is derived directly from this equivalent formulation.

3.3 Applying numerical method to the main problem

In this section, we address the numerical solution of problem (15). First, we consider the following change of variable:

$$\begin{cases} v(\chi,\rho) = \xi_\chi(\chi,\rho), \\ v_\chi(\chi,\rho) = \xi_{\chi\chi}(\chi,\rho), \end{cases}$$

where function $v(\chi,\rho)$ is used as an intermediate function to maintain the continuity of the derivatives of $\xi(\chi,\rho)$ during the discretization. In this case, the problem (15) can be rewritten as the following equation:

$$\begin{aligned}
&{}_0^C D_\rho^\alpha \xi(\chi,\rho) = v_\chi(\chi,\rho) + \mathcal{F}(\xi(\chi,\rho)) + \mathcal{G}(\chi,\rho), \quad (\chi,\rho) \in \varDelta_i \times (0,P], \\
&v(\chi,\rho) = \xi_\chi(\chi,\rho), \quad \chi \in \varDelta_i, \\
&{}_0^C D_\rho^{\frac{\alpha}{2}} v(\chi,\rho) = v_\chi(\chi,\rho) + \mathcal{F}(\xi(\chi,\rho)) + \mathcal{G}(\chi,\rho), \quad \chi \in \varDelta_-, \\
&v(\chi,\rho) = \xi_\chi(\chi,\rho), \quad \chi \in \varDelta_-, \\
&{}_0^C D_\rho^{\frac{\alpha}{2}} v(\chi,\rho) = -(v_\chi(\chi,\rho) + \mathcal{F}(\xi(\chi,\rho)) + \mathcal{G}(\chi,\rho)), \quad \chi \in \varDelta_+, \qquad (24)
\end{aligned}$$

$$
\begin{aligned}
&v(\chi,\rho)=\xi_\chi(\chi,\rho), \quad \chi\in\Delta_+\\
&\xi(\chi,0)=\varphi(\chi), \quad \chi\in\Delta_i,\\
&\xi(0,\rho)=\phi(\rho), \quad \rho>0.
\end{aligned}
$$

We observe that problem (1) is equivalent to problem (24), as their solutions coincide. Thus, we formulate the following lemma to establish the uniqueness of the solution to problem (24).

Remark 1. (a) In the numerical implementation, the nonlinear term $\mathcal{F}(\xi_i^k)$ is replaced by its previous-time value $\mathcal{F}(\xi_i^{k-1})$. This semi-implicit (time-lagging) treatment linearizes the discrete system at each time-step and significantly reduces the computational cost. (b) To analyze the effect of this replacement, we define $T_i^k=\mathcal{F}(\xi_i^k)-\mathcal{F}(\xi_i^{k-1})$. Under the Lipschitz continuity condition $|\mathcal{F}(\xi_i^k)-\mathcal{F}(\xi_i^{k-1})|\le L|\xi_i^k-\xi_i^{k-1}|$, it follows that $|T_i^k|\le L|\xi_i^k-\xi_i^{k-1}|$. Hence the lagging error is of higher order and does not affect the overall accuracy, stability, or convergence of the proposed scheme.

Lemma 2. Assume $\xi(\chi,\rho)\in C^{4,6}([I_-,I_+]\times[0,P])$, and let the temporal grid be $\rho_k=k\varrho$. Suppose the ghost value is chosen so that $\xi^{-1}=\xi^0+\mathcal{O}(\varrho^3)$ this holds if $\partial_\rho\xi(\chi,0)=\partial_\rho^2\xi(\chi,0)=0$. Then the local truncation error $\mathcal{R}_i^k$ of the scheme (24) satisfies

$$\mathcal{R}_i^k=\mathcal{O}(\varrho^{3-\alpha}+h^2),$$

uniformly for $0\le i\le M$ and $1\le k\le N$.

Proof. The smoothness assumption $\xi\in C_\chi^4C_\rho^6([I_-,I_+]\times[0,P])$ ensures that the remainder terms in the temporal Taylor expansions are uniformly bounded with respect to both χ and ρ. Moreover, since the temporal grid is uniform ($\rho_k=k\varrho$), the mean value theorem yields

$$
\begin{aligned}
\partial_\rho\xi(\chi_i,\rho_j)&=\partial_\rho\xi(\chi_i,\rho_k)+O(|\rho_j-\rho_k|)\\
&=\partial_\rho\xi(\chi_i,\rho_k)+O(\varrho),
\end{aligned}
$$

and a similar relation holds for $\partial_\rho^2\xi$. Hence, replacing ρ_j by ρ_k inside the discrete fractional sums introduces an additional term of order $O(\varrho^{3-\alpha})$, which is absorbed into the overall truncation error. The choice $\xi_{-1}=\xi_0+O(\varrho^3)$, corresponding to the conditions $\xi_\rho(\chi,0)=\xi_{\rho\rho}(\chi,0)=0$, eliminates any lower–order boundary contributions. We then proceed with the Taylor expansions for fixed i,k and each $j=0,\ldots,k-1$.

$$
\begin{cases}
\xi_i^{j+1} - \xi_i^{j-1} = 2\varrho\, \partial_\rho \xi(\chi_i,\rho_j) + \dfrac{2\varrho^3}{6}\partial_\rho^3 \xi(\chi_i,\rho_j) + \mathcal{O}(\varrho^5),\\
\xi_i^{j+1} - 2\xi_i^{j} + \xi_i^{j-1} = \varrho^2\, \partial_\rho^2 \xi(\chi_i,\rho_j) + \mathcal{O}(\varrho^4),\\
\xi_{i+1}^{k} - 2\xi_i^{k} + \xi_{i-1}^{k} = h^2\, \partial_\chi^2 \xi(\chi_i,\rho_k) + \mathcal{O}(h^4).
\end{cases}
\tag{25}
$$

Recall the discrete Caputo approximation used in the scheme (22):

$$
\begin{aligned}
{}_0^C D_\rho^\alpha \xi(\rho)|_{\rho=\rho_k} = & \frac{\varrho^{-\alpha}}{\Gamma(3-\alpha)} \sum_{j=0}^{k-1} (\omega_{1,k-j}(\xi^{j+1} - \xi^{j-1}) \\
& + \omega_{2,k-j}(\xi^{j+1} - 2\xi^{j} + \xi^{j-1})) + O(\varrho^{3-\alpha}),
\end{aligned}
$$

where the remainder $\mathcal{O}(\varrho^{3-\alpha})$ originates from integrating the higher-order terms of the Taylor expansions against the kernel $(\rho_k - \vartheta)^{-\alpha}$ on each temporal subinterval; under the stated smoothness the constant in this bound is uniform in k (see [7, Lemma 2.1]). Substitute the expansions (25) into the discrete Caputo sum to obtain

$$
\begin{aligned}
& \frac{\varrho^{-\alpha}}{\Gamma(3-\alpha)} \sum_{j=0}^{k-1} \Big(\omega_{1,k-j}(\xi_i^{j+1} - \xi_i^{j-1}) + \omega_{2,k-j}(\xi_i^{j+1} - 2\xi_i^{j} + \xi_i^{j-1}) \Big) \\
&= \frac{\varrho^{-\alpha}}{\Gamma(3-\alpha)} \sum_{j=0}^{k-1} \Big(2\varrho\, \omega_{1,k-j}\, \partial_\rho \xi(\chi_i,\rho_j) + \varrho^2 \omega_{2,k-j}\, \partial_\rho^2 \xi(\chi_i,\rho_j) \Big) + \mathcal{O}(\varrho^{3-\alpha}).
\end{aligned}
$$

By the regularity of $\partial_\rho \xi$ and $\partial_\rho^2 \xi$ on $[0,\rho_k]$ and using the boundedness and positivity properties of the weights $\{\omega_{1,m}\}, \{\omega_{2,m}\}$ 1, we may replace the temporal arguments ρ_j by ρ_k up to a temporal interpolation error of order $\mathcal{O}(\varrho)$ inside the sums. Consequently,

$$
\frac{\varrho^{-\alpha}}{\Gamma(3-\alpha)} \Big(2\varrho \partial_\rho \xi(\chi_i,\rho_k) \sum_{j=0}^{k-1} \omega_{1,k-j} + \varrho^2 \partial_\rho^2 \xi(\chi_i,\rho_k) \sum_{j=0}^{k-1} \omega_{2,k-j} \Big) + \mathcal{O}(\varrho^{3-\alpha}).
$$

A direct comparison with the continuous Caputo derivative shows that the leading discrete terms reproduce the continuous operator up to the $\mathcal{O}(\varrho^{3-\alpha})$ remainder (this is the standard consistency calculation for the chosen weights; the details follow from the definition of $\omega_{1,n}, \omega_{2,n}$ and standard quadrature estimates). Together with the spatial discretization error $\mathcal{O}(h^2)$ from (25), we obtain a bound for the local truncation error of the fully discrete scheme:

$$
|\mathcal{R}_i^k| \le C_1 \big(\varrho^{3-\alpha} + h^2 \big),
$$

for some constant $C_1 > 0$ independent of ϱ, h, uniformly in i, k. Finally, the hypothesis $\xi_{-1} = \xi_0 + \mathcal{O}(\varrho^3)$ guarantees that no lower-order boundary-term arising from the ghost value degrades the stated order. Therefore $\mathcal{R}_i^k = \mathcal{O}(\varrho^{3-\alpha} + h^2)$, which proves the lemma. $\square$

Assume that $\xi(\chi, \rho) \in C^{4,6}_{\chi,\rho}(\mathbb{R})$, and define the discrete values $\xi_i^k = \xi(\chi_i, \rho_k)$, $V_i^k = v(\chi_i, \rho_k)$ and source term $g_i^k = \mathcal{G}(\chi_i, \rho_k)$, function $f(\xi(\chi_i, \rho_{k-1}))$ is defined as $\mathcal{F}(\xi(\chi_i, \rho_{k-1}))$. By employing the fractional derivative approximation formula given in relation (22) and using Lemma 2, together with Taylor expansion, we obtain

$$\begin{aligned}
&{}_0^C D_\rho^\alpha \xi^k_{i+\frac{1}{2}} = \sigma_\chi V^k_{i+\frac{1}{2}} + \mathcal{F}(\xi^{k-1}_{i+\frac{1}{2}}) + \mathcal{G}^k_{i+\frac{1}{2}} + R^k_{i+\frac{1}{2}},\\
&V^k_{i+\frac{1}{2}} = \sigma_\chi \xi^k_{i+\frac{1}{2}} + Z^k_{i+\frac{1}{2}},\\
&{}_0^C D^{\frac{\alpha}{2}} V_0^k = \left(\sigma_\chi V_0^k + \mathcal{F}(\xi_0^{k-1}) + \mathcal{G}_0^k\right) + T^k,\\
&V_0^k = \sigma_\chi \xi_0^k + A^k,\\
&{}_0^C D^{\frac{\alpha}{2}} V_M^k = -\left(\sigma_\chi V_M^k + \mathcal{F}(\xi_M^{k-1}) + \mathcal{G}_M^k\right) + W^k,\\
&V_M^k = \sigma_\chi \xi_M^k + Q^k,\\
&\xi_i^0 = \varphi(\chi_i), \qquad \chi \in \mathit{\Delta}_i,\\
&\xi_0^k = \phi(\rho_k), \qquad \rho > 0,
\end{aligned} \tag{26}$$

where the remainder functions are denoted by R, Z, T, A, W, and Q. There exists a positive constant C_0 such that [6]

$$\begin{aligned}
&|R^k_{i+\frac{1}{2}}| \le C_0\left(\varrho^{3-\alpha} + h^2\right), \quad |Z^k_{i+\frac{1}{2}}| \le C_0 h^2, \quad |T^k| \le C_0(\varrho^{3-\frac{\alpha}{2}} + h^2),\\
&|A^k| \le C_0 h^2, \qquad |W^k| \le C_0(\varrho^{3-\frac{\alpha}{2}} + h^2), \quad |Q^k| \le C_0 h^2,
\end{aligned} \tag{27}$$

By assuming that $\xi(\chi, \rho) \in C^{4,6}_{\chi,\rho}(\mathbb{R})$ and applying the fractional derivative approximation in (22) together with Lemma 2 and the Taylor expansion, the discrete formulation (26) is obtained. The remainder terms, denoted by R, Z, T, A, W, and Q, represent higher–order truncation errors, whose magnitudes are bounded as in (27). Since these terms are of order $\mathcal{O}(\varrho^{3-\alpha} + h^2)$ or smaller, their effects can be neglected in the implementation stage $R = Z = T = A = W = Q = 0$. Consequently, the simplified and implementable finite difference scheme with accuracy $\mathcal{O}(\varrho^{3-\alpha} + h^2)$ and guaranteed stability is obtained, as presented in (28).

$$\begin{aligned}
&{}_0^C D_\rho^\alpha \xi^k_{i+\frac{1}{2}} = \sigma_\chi v^k_{i+\frac{1}{2}} + f(\xi^{k-1}_{i+\frac{1}{2}}) + g^k_{i+\frac{1}{2}},\\
&v^k_{i+\frac{1}{2}} = \sigma_\chi \xi^k_{i+\frac{1}{2}},
\end{aligned}$$

$$
\begin{aligned}
&{}_0^C D_\rho^{\frac{\alpha}{2}} v_0^k = \left(\sigma_\chi v_0^k + f(\xi_0^{k-1}) + g_0^k\right), \\
&v_0^k = \sigma_\chi \xi_0^k, \\
&{}_0^C D_\rho^{\frac{\alpha}{2}} v_M^k = -\left(\sigma_\chi v_M^k + f(\xi_M^{k-1}) + g_M^k\right), \\
&v_M^k = \sigma_\chi \xi_M^k, \\
&\xi_i^0 = \varphi(\chi_i), \qquad \chi \in \Delta_i, \\
&\xi_0^k = \phi(\rho_k), \qquad \rho > 0.
\end{aligned} \tag{28}
$$

For the interior grid points $1 \leqslant i \leqslant M-1$, the classical second-order central difference approximation is applied for the spatial derivative, which provides an accuracy of order $\mathcal{O}(h^2)$. However, at the boundary points χ_0 and χ_M, the external function values ξ_{-1} and ξ_{M+1} are not available, and thus the standard central difference formula cannot be directly employed. To preserve the second-order spatial accuracy and maintain the consistency of the numerical solution, Lemma 3 constructs suitable boundary approximations by expressing the spatial derivatives at the boundaries in terms of the known nodal values and the exact ABCs derived in Section 2. These boundary relations are incorporated into Theorem 1, where the complete discrete system of equations is established by combining the interior scheme (28) with the boundary approximations from Lemma 3. Consequently, Theorem 3.4 ensures that the number of algebraic equations equals the number of unknowns, making the proposed finite difference formulation fully discrete and directly implementable. We approximate the second-order integer derivative as follows:

Lemma 3. Assume that $\xi(\chi) \in C^4[I_-, I_+]$, that $h = \frac{I_+ - I_-}{M}$, and that M is a given positive integer. Then

$$
\begin{aligned}
&\xi''(\chi_0) - \frac{2}{h}\left(\frac{\xi(\chi_1) - \xi(\chi_0)}{h} - \xi'(\chi_0)\right) = -\frac{h}{3}\xi^{(3)}(\chi_0 + \theta_1 h), \quad \theta_1 \in (0,1), \\
&\xi''(\chi_M) - \frac{2}{h}\left(\xi'(\chi_M) - \frac{\xi(\chi_M) - \xi(\chi_{M-1})}{h}\right) = \frac{h}{3}\xi^{(3)}(\chi_M - \theta_2 h), \quad \theta_2 \in (0,1).
\end{aligned} \tag{29}
$$

Proof. Lemma 3 can be easily proven using Taylor's theorem. □

Theorem 1. for $1 \leq i \leq M-1$, $1 \leq k \leq N$ the finite difference scheme (28) is equivalent to

$$
\begin{aligned}
\frac{1}{2}\left({}_0^C D_\rho^\alpha \xi_{i-\frac{1}{2}}^k + {}_0^C D_\rho^\alpha \xi_{i+\frac{1}{2}}^k\right) =& \sigma_\chi^2 \xi_i^k + \frac{1}{2}\left(f(\xi_{i-\frac{1}{2}}^{k-1}) + f(\xi_{i+\frac{1}{2}}^{k-1})\right) \\
&+ \frac{1}{2}\left(g_{i-\frac{1}{2}}^k + g_{i+\frac{1}{2}}^k\right), \\
{}_0^C D_\rho^\alpha \xi_{\frac{1}{2}}^k =& \frac{2}{h}\left(\sigma_\chi \xi_{\frac{1}{2}}^k - {}_0^C D_\rho^{\frac{\alpha}{2}} \xi_0^k + f(\xi_0^{k-1})\right) + g_{\frac{1}{2}}^k, \\
{}_0^C D_\rho^\alpha \xi_{M-\frac{1}{2}}^k =& \frac{2}{h}\left(-{}_0^C D_\rho^{\frac{\alpha}{2}} \xi_M^k - \sigma_\chi \xi_{M+\frac{1}{2}}^k - f(\xi_M^{k-1})\right) + g_{M-\frac{1}{2}}^k,
\end{aligned}
$$

$$\begin{aligned} \xi_i^0 =& \xi(\chi_i), \quad 0 \le i \le M, \\ \xi_0^k =& \varphi(\rho_k), \end{aligned} \tag{30}$$

and

$$\begin{aligned} v_0^k &= \sigma_\chi \xi_{\frac{1}{2}}^k - \frac{h}{2}\left({}_0^C D_\rho^\alpha \xi_{\frac{1}{2}}^k - f(\xi_0^{k-1}) - g_{\frac{1}{2}}^k\right), \\ v_M^k &= \sigma_\chi \xi_{M-\frac{1}{2}}^k + \frac{h}{2}\left({}_0^C D_\rho^\alpha \xi_{M-\frac{1}{2}}^k - f(\xi_M^{k-1}) - g_{M-\frac{1}{2}}^k\right), \\ v_i^k &= \sigma_\chi \xi_{i-\frac{1}{2}}^k + \frac{h}{2}\left({}_0^C D_\rho^\alpha \xi_{i-\frac{1}{2}}^k - f(\xi_i^{k-1}) - g_{i-\frac{1}{2}}^k\right), \quad 1 \le i \le M, 1 \le k \le N. \end{aligned}$$

Proof. We start from the discrete relations at the half-grid points, as presented in (28) of the manuscript:

$$\frac{1}{2}\big(v_{i+1}^k - v_i^k\big) = \frac{h}{2}\Big({}_0^C D_\rho^\alpha \xi_{i+\frac{1}{2}}^k - \mathcal{F}(\xi_{i+\frac{1}{2}}^{k-1}) - \mathcal{G}_{i+\frac{1}{2}}^k\Big), 0 \le i \le M-1,\ 1 \le k \le N, \tag{31}$$

$$v_{i+\frac{1}{2}}^k = \sigma_\chi\, \xi_{i+\frac{1}{2}}^k. \tag{32}$$

Here we employ the semi-implicit treatment $\mathcal{F}(\xi_i^k) \mapsto \mathcal{F}(\xi_i^{k-1})$ and omit the higher-order remainder terms (see the bounds in (27)), the neglected terms are of order $\mathcal{O}(\varrho^{3-\alpha} + h^2)$. To derive an explicit expression for v_{i+1}^k, we add (31) and (32) evaluated at the same half-point. Using the standard identity $v_{i+\frac{1}{2}}^k = \frac{1}{2}(v_{i+1}^k + v_i^k)$, which follows from the definition of the half-grid variables, we obtain after simple algebra

$$v_{i+1}^k = \sigma_\chi\, \xi_{i+\frac{1}{2}}^k + \frac{h}{2}\Big({}_0^C D_\rho^\alpha \xi_{i+\frac{1}{2}}^k - \mathcal{F}(\xi_{i+\frac{1}{2}}^{k-1}) - \mathcal{G}_{i+\frac{1}{2}}^k\Big).$$

Shifting the index $i \mapsto i-1$ yields the equivalent relation

$$v_i^k = \sigma_\chi\, \xi_{i-\frac{1}{2}}^k + \frac{h}{2}\Big({}_0^C D_\rho^\alpha \xi_{i-\frac{1}{2}}^k - \mathcal{F}(\xi_{i-\frac{1}{2}}^{k-1}) - \mathcal{G}_{i-\frac{1}{2}}^k\Big), \qquad 1 \le i \le M. \tag{33}$$

Next, to obtain an expression for v_i^k in terms of the right half-point, we use (31) at index i together with (32) at $i + \frac{1}{2}$. Eliminating the difference $v_{i+1}^k - v_i^k$ between these two relations gives

$$v_i^k = \sigma_\chi\, \xi_{i+\frac{1}{2}}^k - \frac{h}{2}\Big({}_0^C D_\rho^\alpha \xi_{i+\frac{1}{2}}^k - \mathcal{F}(\xi_{i+\frac{1}{2}}^{k-1}) - \mathcal{G}_{i+\frac{1}{2}}^k\Big), \qquad 0 \le i \le M-1. \tag{34}$$

Now, combine (33) and (34) for interior indices $1 \le i \le M-1$. Adding the two expressions for v_i^k and dividing by two yields

$$\frac{1}{2}\Big({}_0^C D_\rho^\alpha \xi_{i-\frac{1}{2}}^k + {}_0^C D_\rho^\alpha \xi_{i+\frac{1}{2}}^k\Big) = \sigma_\chi^2 \xi_i^k + \frac{1}{2}\Big(\mathcal{F}(\xi_{i-\frac{1}{2}}^{k-1}) + \mathcal{F}(\xi_{i+\frac{1}{2}}^{k-1})\Big) + \frac{1}{2}\Big(\mathcal{G}_{i-\frac{1}{2}}^k + \mathcal{G}_{i+\frac{1}{2}}^k\Big),$$

which is exactly the interior equation stated in Theorem 1. In the interior domain, the nonlinear term $\mathcal{F}(\xi_i^k)$ is treated semi-implicitly, $\mathcal{F}(\xi_i^k)$ is replaced by its previous time level $\mathcal{F}(\xi_i^{k-1})$ to ensure numerical stability and to avoid solving a nonlinear system at each step. However, in the boundary relations derived from the discrete ABCs, this term naturally appears with the current time index k, since those relations are obtained directly from the continuous ABC operators and therefore do not involve any time-lagging approximation. This difference in the treatment of $\mathcal{F}$ does not affect the overall consistency, as both approximations preserve the same truncation order $\mathcal{O}(\varrho^{3-\alpha} + h^2)$ (27). Finally, to derive the right boundary formula, substitute (33) with $i = M$ and use the ABC given in the manuscript:

$$ {}_0^C D_\rho^{\alpha/2} v_M^k = -\big(\sigma_\chi v_M^k + \mathcal{F}(\xi_M^{k-1}) + \mathcal{G}_M^k\big), \qquad v_M^k = \sigma_\chi \xi_M^k. $$

Note that ${}_0^C D_\rho^{\alpha/2} v_M^k = {}_0^C D_\rho^{\alpha/2}(\sigma_\chi \xi_M^k)$. Substituting this relation and rearranging terms gives

$$ {}_0^C D_\rho^{\alpha} \xi_{M-\frac{1}{2}}^k = \frac{2}{h}\Big(- {}_0^C D_\rho^{\alpha/2}(\sigma_\chi \xi_M^k) - \sigma_\chi \xi_{M+\frac{1}{2}}^k - \mathcal{F}(\xi_M^{k-1})\Big) + \mathcal{G}_{M-\frac{1}{2}}^k. $$

Here $\xi_{M+\frac{1}{2}}^k$ denotes the boundary-adjacent value treated via the discrete ABC approximation Lemma 3. The left boundary relation is obtained analogously. Combining the interior and boundary equations shows that the total number of discrete equations matches the number of unknown nodal values, so the fully discrete system is well-posed and can be solved uniquely at each time level. This completes the proof. □

4 Stability and convergence of the numerical method

In this section, we present several preliminary lemmas that will be essential for establishing the stability and convergence of the proposed finite difference scheme. These lemmas provide useful discrete inequalities and auxiliary estimates that simplify the forthcoming analysis.

Lemma 4. [5, 11] Suppose the network function $\xi = \{\xi^k \mid 0 \le k \le N\}$ is defined on the temporal grid Π_ϱ. Then, the following inequality holds:

$$ \varrho \sum_{k=1}^{n} \left({}_0^C D_\rho^{\alpha} \xi^k\right) \xi^k \ge \frac{\rho_n^{-\alpha}}{2\Gamma(1-\alpha)} \varrho \sum_{k=1}^{n} \left(\xi^k\right)^2 - \frac{\rho_n^{1-\alpha}}{2\Gamma(2-\alpha)} \left(\xi^0\right)^2, \quad 1 \le n \le N, \tag{35} $$

where ${}_{0}^{C}D_{\rho}^{\alpha}\xi^{k}$ for $k \geq 1$ is defined according to the relation (22). This lemma plays a crucial role in establishing the positivity and coercivity of the discrete Caputo operator, which are essential properties for the stability and convergence analysis of fractional time-stepping schemes.

Lemma 5. [5] Let ξ be a grid function defined on the spatial grid Π_h with $\xi_0 = 0$. Then the following discrete inverse inequality holds:

$$\|\xi^k\|_\infty^2 \leq C\,\|\sigma_\chi \xi^k\|^2, \tag{36}$$

where C is a positive constant independent of h.

The above lemmas provide the fundamental discrete estimates required for analyzing the stability and convergence properties of the proposed scheme.

Theorem 2 (Initial estimate)**.** Assume that $\{\xi_i^k : 0 \leq i \leq M,\ 0 \leq k \leq N\}$ is the grid solution of the discrete scheme (37)–(44), with the notation $\rho_n = n\varrho$ and the discrete norms $\|\cdot\|$ (discrete L^2) and $\|\cdot\|_\infty$ (discrete supremum). Moreover,

$$
\begin{aligned}
&{}_{0}^{C}D_{\rho}^{\alpha}\xi_{i+\frac{1}{2}}^{k} = \sigma_\chi v_{i+\frac{1}{2}}^{k} + f(\xi_{i+\frac{1}{2}}^{k-1}) + g_{i+\frac{1}{2}}^{k}, \qquad 0 \leqslant i \leqslant M-1, &(37)\\
&v_{i+\frac{1}{2}}^{k} = \sigma_\chi \xi_{i+\frac{1}{2}}^{k} + z_{i+\frac{1}{2}}^{k} \qquad 0 \leqslant i \leqslant M-1, &(38)\\
&{}_{0}^{C}D_{\rho}^{\frac{\alpha}{2}} v_0^k = \sigma_\chi v_0^k + f(\xi_0^{k-1}) + g_0^k + t^k, &(39)\\
&v_0^k = \sigma_\chi \xi_0^k + a^k, &(40)\\
&{}_{0}^{C}D_{\rho}^{\frac{\alpha}{2}} v_M^k = -\sigma_\chi v_M^k - f(\xi_M^{k-1}) - g_M^k + w^k, &(41)\\
&v_M^k = \sigma_\chi \xi_M^k + q^k, &(42)\\
&\xi_i^0 = \varphi(\chi_i), \qquad \chi \in \mathit{\Delta}_i, &(43)\\
&\xi_0^k = 0, \qquad \rho > 0. &(44)
\end{aligned}
$$

Suppose furthermore that the remainder terms $z_{i+\frac{1}{2}}^{k}, t^k, a^k, w^k, q^k$ satisfy the bounds from Lemma 2 and relation (27):

$$|z_{i+\frac{1}{2}}^{k}| \leq C_0 h^2, \quad |a^k|, |q^k| \leq C_0 h^2, \quad |t^k|, |w^k| \leq C_0(\varrho^{3-\frac{\alpha}{2}} + h^2),$$

for some $C_0 > 0$ independent of h, ϱ. Let

$$\mu_n := \frac{\rho_n^{-\alpha}}{\Gamma(1-\alpha)}, \qquad 1 \leq n \leq N.$$

Then for every $1 \leq n \leq N$ it holds that

$$\begin{aligned}\varrho\sum_{k=1}^{n}\|\xi^k\|_\infty^2+\mu_n\,\varrho\sum_{k=1}^{n}\|\xi^k\|^2\leq &C_1\|\xi^0\|^2+C_2\varrho\sum_{k=1}^{n}(f(\xi^{k-1}),\xi^k)\\ &+C_3\varrho\sum_{k=1}^{n}\|g^k\|^2+C_4\varrho\sum_{k=1}^{n}(q^k)^2\\ &+C_5\varrho\sum_{k=1}^{n}\big((\xi_M^k)^2+(\sigma_\chi\xi_M^k)^2\big),\end{aligned} \tag{45}$$

where $C_1,\dots,C_5>0$ are constants depending only on α, C_0 the remainder bounds and universal constants but independent of h,ϱ and n.

Proof. Using the discrete inner product and applying relations (37)–(38), we obtain

$$\begin{aligned}({}_0^CD_\rho^\alpha\xi^k,\,\xi^k)&=(\sigma_\chi v^k,\,\xi^k)+(f(\xi^{k-1}),\,\xi^k)+(g^k,\,\xi^k),\\ (v^k,\,v^k)&=(\sigma_\chi\xi^k,\,v^k)+(z_{i+\frac12}^k,\,v^k),\qquad 1\leq k\leq N.\end{aligned} \tag{46}$$

Adding these two relations gives

$$\begin{aligned}({}_0^CD_\rho^\alpha\xi^k,\,\xi^k)+\|v^k\|^2=&(\sigma_\chi v^k,\,\xi^k)+(\sigma_\chi\xi^k,\,v^k)+(f(\xi^{k-1}),\,\xi^k)+(g^k,\,\xi^k)\\ &+(z_{i+\frac12}^k,\,v^k),\qquad 1\leq k\leq N.\end{aligned} \tag{47}$$

Next, using the discrete integration-by-parts identity together with the boundary conditions (42) and (44), we have

$$\begin{aligned}(\sigma_\chi\xi^k,\,v^k)+(\sigma_\chi v^k,\,\xi^k)&=h\sum_{i=1}^{M}\left[(\sigma_\chi\xi_{i-\frac12}^k)v_{i-\frac12}^k+(\sigma_\chi v_{i-\frac12}^k)\xi_{i-\frac12}^k\right]\\ &=\xi_M^kv_M^k-\xi_0^kv_0^k=\xi_M^k(\sigma_\chi\xi_M^k+q^k),\end{aligned} \tag{48}$$

since $\xi_0^k=0$ for all k. Combining (47) and (48) yields

$$\begin{aligned}({}_0^CD_\rho^\alpha\xi^k,\,\xi^k)+\|v^k\|^2=&(f(\xi^{k-1}),\,\xi^k)+(g^k,\,\xi^k)+\xi_M^k\sigma_\chi\xi_M^k+\xi_M^kq^k\\ &+(z_{i+\frac12}^k,\,v^k),\qquad 1\leq k\leq N.\end{aligned} \tag{49}$$

Multiplying both sides of (49) by ϱ, summing over $k=1,\dots,n$, and applying Lemma 4, we obtain

$$\frac{\rho_n^{-\alpha}}{2\Gamma(1-\alpha)}\,\varrho\sum_{k=1}^{n}\|\xi^k\|^2+\varrho\sum_{k=1}^{n}\|v^k\|^2$$

$$\le \frac{\rho_n^{1-\alpha}}{2\Gamma(2-\alpha)}\,\|\xi^0\|^2 + \varrho\sum_{k=1}^{n}(f(\xi^{k-1}),\,\xi^k) + \varrho\sum_{k=1}^{n}(g^k,\,\xi^k)$$

$$+\,\varrho\sum_{k=1}^{n}\xi_M^k\,\sigma_\chi\xi_M^k + \varrho\sum_{k=1}^{n}(z_{i+\frac{1}{2}}^k,\,v^k) + \varrho\sum_{k=1}^{n}\xi_M^k\,q^k, \quad 1\le n\le N. \tag{50}$$

Applying the Cauchy–Schwarz and Young inequalities to the right-hand side of (50) yields the following estimate:

$$\begin{aligned}
&\frac{\rho_n^{-\alpha}}{2\Gamma(1-\alpha)}\,\varrho\sum_{k=1}^{n}\|\xi^k\|^2 + \varrho\sum_{k=1}^{n}\|v^k\|^2\\
&\quad\le \frac{\rho_n^{1-\alpha}}{2\Gamma(2-\alpha)}\,\|\xi^0\|^2 + \varrho\sum_{k=1}^{n}(f(\xi^{k-1}),\,\xi^k)\\
&\qquad+\varrho\sum_{k=1}^{n}\left(\frac{\rho_n^{-\alpha}}{4\Gamma(1-\alpha)}\,\|\xi^k\|^2 + \rho_n^{\alpha}\Gamma(1-\alpha)\,\|g^k\|^2\right)\\
&\qquad+\varrho\sum_{k=1}^{n}\left(\frac{1}{2}\|v^k\|^2 + \frac{1}{2}\|z_{i+\frac{1}{2}}^k\|^2\right) + \varrho\sum_{k=1}^{n}\left(\frac{1}{2}(\xi_M^k)^2 + \frac{1}{2}(q^k)^2\right)\\
&\qquad+\varrho\sum_{k=1}^{n}\left(\frac{1}{2}(\xi_M^k)^2 + \frac{1}{2}(\sigma_\chi\xi_M^k)^2\right), \quad 1\le n\le N.
\end{aligned}\tag{51}$$

Using the estimate (51) and moving the small left-hand terms to the left, we obtain

$$\begin{aligned}
&\frac{\rho_n^{-\alpha}}{4\Gamma(1-\alpha)}\,\varrho\sum_{k=1}^{n}\|\xi^k\|^2 + \frac{1}{2}\,\varrho\sum_{k=1}^{n}\|v^k\|^2\\
&\quad\le \frac{\rho_n^{1-\alpha}}{2\Gamma(2-\alpha)}\,\|\xi^0\|^2 + \varrho\sum_{k=1}^{n}(f(\xi^{k-1}),\,\xi^k)\\
&\qquad+\rho_n^{\alpha}\Gamma(1-\alpha)\,\varrho\sum_{k=1}^{n}\|g^k\|^2 + \frac{1}{2}\,\varrho\sum_{k=1}^{n}\|z_{i+\frac{1}{2}}^k\|^2 + \varrho\sum_{k=1}^{n}\left(\frac{1}{2}(q^k)^2 + (\xi_M^k)^2\right)\\
&\qquad+\frac{1}{2}\,\varrho\sum_{k=1}^{n}(\sigma_\chi\xi_M^k)^2,
\end{aligned}\tag{52}$$

for every $1\le n\le N$. Using relation (38) together with Lemma 5, we have the pointwise bound

$$\|\xi^k\|_\infty^2 \le \|\sigma_\chi\xi^k\|^2 = \|v^k - z_{i+\frac{1}{2}}^k\|^2 \le 2\|v^k\|^2 + 2\|z_{i+\frac{1}{2}}^k\|^2, \qquad 1\le k\le N. \tag{53}$$

Now, multiply (53) by ϱ and sum over $k=1,\dots,n$, then combine with (52). Using the fact that $\frac{1}{2}\varrho\sum_{k=1}^{n}\|v^k\|^2$ appears on the left of (52), we obtain after elementary algebra the inequality

$$
\begin{aligned}
&\varrho \sum_{k=1}^{n} \|\xi^k\|_\infty^2 + \frac{\rho_n^{-\alpha}}{\Gamma(1-\alpha)}\, \varrho \sum_{k=1}^{n} \|\xi^k\|^2 - 4\varrho \sum_{k=1}^{n} (\xi_M^k)^2 - 2\varrho \sum_{k=1}^{n} (\sigma_\chi \xi_M^k)^2 \\
&\le \frac{2\rho_n^{1-\alpha}}{\Gamma(2-\alpha)}\, \|\xi^0\|^2 + 4\varrho \sum_{k=1}^{n} (f(\xi^{k-1}),\, \xi^k) + 4\rho_n^{\alpha}\Gamma(1-\alpha)\, \varrho \sum_{k=1}^{n} \|g^k\|^2 \\
&+ \quad C_z\, \varrho \sum_{k=1}^{n} \|z_{i+\frac{1}{2}}^k\|^2 + \varrho \sum_{k=1}^{n} (q^k)^2,
\end{aligned} \tag{54}
$$

for every $1 \le n \le N$, where $C_z > 0$ is a numerical constant (here one may take $C_z = 4$). Finally, by introducing the notation

$$
\mu_n = \frac{\rho_n^{-\alpha}}{\Gamma(1-\alpha)},
$$

and substituting this definition into (54), we simplify the inequality as

$$
\begin{aligned}
&\varrho \sum_{k=1}^{n} \|\xi^k\|_\infty^2 + \mu_n\, \varrho \sum_{k=1}^{n} \|\xi^k\|^2 - 4\varrho \sum_{k=1}^{n} (\xi_M^k)^2 - 2\varrho \sum_{k=1}^{n} (\sigma_\chi \xi_M^k)^2 \\
&\qquad \le \frac{2\mu_n \rho_n}{1-\alpha}\, \|\xi^0\|^2 + 4\varrho \sum_{k=1}^{n} (f(\xi^{k-1}), \xi^k) + \frac{4}{\mu_n}\, \varrho \sum_{k=1}^{n} \|g^k\|^2 + 2\varrho \sum_{k=1}^{n} (q^k)^2.
\end{aligned} \tag{55}
$$

This inequality coincides precisely with relation (45), which completes the proof of Theorem 2. □

The purpose of Theorem 2 (Initial Estimate) is to establish a discrete *a priori* energy bound for the numerical solution. This estimate ensures that the grid solution $\{\xi_i^k\}$ remains uniformly bounded at all temporal levels and that the discrete ABCs do not introduce instability into the system. Therefore, this theorem provides the theoretical foundation for the subsequent stability and convergence analysis of the proposed numerical method.

Theorem 3 (Stability)**.** Based on the discrete scheme (30) and under the assumptions of Theorem 2, the proposed finite difference method is *unconditionally stable*. Specifically, let ξ_i^k $(0 \le i \le M,\ 1 \le k \le N)$ denote the numerical solution with homogeneous initial data $\varphi(\rho_k) = 0$ for all $1 \le k \le N$. Then, the following stability estimate holds:

$$
\begin{aligned}
&\varrho \sum_{k=1}^{n} \|\xi^k\|_\infty^2 + \frac{\mu_n}{4}\, \varrho \sum_{k=1}^{n} \|\xi^k\|^2 - 2\varrho \sum_{k=1}^{n} (\xi_M^k)^2 - \varrho \sum_{k=1}^{n} (\sigma_\chi \xi_M^k)^2 \\
&\qquad \le \frac{\mu_n \rho_n}{2(1-\alpha)}\, \|\xi^0\|^2 + \varrho \sum_{k=1}^{n} \left(f(\xi^{k-1}), \xi^k\right) + \frac{1}{\mu_n}\, \varrho \sum_{k=1}^{n} \|g^k\|^2,
\end{aligned} \tag{56}
$$

where $\mu_n = \dfrac{\rho_n^{-\alpha}}{\Gamma(1-\alpha)}$, and C_0 denotes the remainder constant introduced in relation (27).

Proof. The proof follows the same energy argument as in Theorem 2. □

In the following, we examine the convergence of the difference method described in relations (37)–(43). We assume that

$$e_i^k = U_i^k - \xi_i^k, \quad \varepsilon_i^k = V_i^k - v_i^k, \quad 0 \le i \le M, \quad 0 \le k \le N,$$

where U_i^k and V_i^k denote the numerical approximations of $\xi(\chi_i, \rho_k)$ and $v(\chi_i, \rho_k)$, respectively.

Theorem 4 (Convergence)**.** Assume that $\xi(\chi, \rho) \in C_{\chi,\rho}^{4,4}([I_-, I_+] \times [0, P])$, and let $\{\xi_i^k \mid 0 \le i \le M,\ 0 \le k \le N\}$ and $\{U_i^k \mid 0 \le i \le M,\ 0 \le k \le N\}$ be the exact and numerical solutions of the problems (15) and (37)–(43), respectively. Then there exists a constant $C_1 > 0$ such that

$$\sqrt{\varrho \sum_{k=1}^{n} \left(\|e^k\|_\infty^2 - 4(e_M^k)^2 - 2(\sigma_\chi e_M^k)^2 + \mu \|e^k\|^2 \right)} \le C_1(\varrho^{3-\alpha} + h^2), \quad 1 \le n \le N, \tag{57}$$

where $e_i^k = U_i^k - \xi_i^k$ is the discretization error. The constant C_1 is given by

$$C_1 = 2C_0 T^{\alpha + \frac{1}{2}} \sqrt{\tfrac{1}{2} + \Gamma(1-\alpha)}, \tag{58}$$

and μ is defined in Theorem 2, while C_0 is specified in (27).

Proof. Following the approach of Theorem 2, we subtract the exact relation (28) from the discrete scheme (26) to obtain the error system:

$$\begin{aligned}
&{}_0^C D_\rho^\alpha e_{i+\frac{1}{2}}^k = \sigma_\chi \varepsilon_{i+\frac{1}{2}}^k + \left(f(U_i^{k-1}) - f(\xi_i^{k-1}) \right) + R_{i+\frac{1}{2}}^k, \quad 0 \le i \le M-1,\ 1 \le k \le N, \\
&\varepsilon_{i+\frac{1}{2}}^k = \sigma_\chi e_{i+\frac{1}{2}}^k + Z_{i+\frac{1}{2}}^k, \\
&{}_0^C D_\rho^{\frac{\alpha}{2}} \varepsilon_0^k = \sigma_\chi \varepsilon_0^k + \left(f(U_0^{k-1}) - f(\xi_0^{k-1}) \right) + T^k, \quad \varepsilon_0^k = \sigma_\chi e_0^k + A^k, \\
&{}_0^C D_\rho^{\frac{\alpha}{2}} \varepsilon_M^k = -\sigma_\chi \varepsilon_M^k - \left(f(U_M^{k-1}) - f(\xi_M^{k-1}) \right) + W^k, \quad \varepsilon_M^k = \sigma_\chi e_M^k + Q^k, \\
&e_i^0 = 0, \quad \chi \in \Delta_i, \qquad e_0^k = 0.
\end{aligned} \tag{59}$$

Applying Theorem 2 to this error system yields

$$\begin{aligned}
&\varrho \sum_{k=1}^{n} \|e^k\|_\infty^2 - 4\varrho \sum_{k=1}^{n} (e_M^k)^2 - 2\varrho \sum_{k=1}^{n} (\sigma_\chi e_M^k)^2 + \mu\varrho \sum_{k=1}^{n} \|e^k\|^2 \\
&\qquad \le \frac{4}{\mu} \varrho \sum_{k=1}^{n} \|R^k\|^2 + 2\varrho \sum_{k=1}^{n} \|Q^k\|^2, \quad 1 \le n \le N.
\end{aligned} \tag{60}$$

Using the remainder bounds from (27), $|R^k|, |Z^k|, |T^k|, |W^k|, |Q^k| \leq C_0(\varrho^{3-\alpha} + h^2)$, we have

$$
\begin{aligned}
&\varrho \sum_{k=1}^{n} \|e^k\|_\infty^2 + \mu\varrho \sum_{k=1}^{n} \|e^k\|^2 - 4\varrho \sum_{k=1}^{n} (e_M^k)^2 - 2\varrho \sum_{k=1}^{n} (\sigma_\chi e_M^k)^2 \\
&\leq 2\rho_n C_0^2 h^4 + \frac{4}{\mu}\big(C_0(\varrho^{3-\alpha} + h^2)\big)^2 \\
&= 2\rho_n C_0^2 h^4 + 4\rho_n^{\alpha+1}\Gamma(1-\alpha)\big(C_0(\varrho^{3-\alpha} + h^2)\big)^2 \\
&\leq 4C_0^2 T^{1+\alpha}\Big(\tfrac{1}{2} + \Gamma(1-\alpha)\Big)(\varrho^{3-\alpha} + h^2)^2.
\end{aligned} \tag{61}
$$

Taking square roots of both sides yields

$$
\begin{aligned}
&\sqrt{\varrho \sum_{k=1}^{n} \big(\|e^k\|_\infty^2 - 4(e_M^k)^2 - 2(\sigma_\chi e_M^k)^2 + \mu\|e^k\|^2\big)} \\
&\leq 2C_0 T^{\alpha+\frac{1}{2}} \sqrt{\tfrac{1}{2} + \Gamma(1-\alpha)}(\varrho^{3-\alpha} + h^2),
\end{aligned} \tag{62}
$$

which proves (57)–(58). □

5 Numerical examples

In this section, two representative numerical examples are provided to comprehensively evaluate the accuracy, stability, and efficiency of the proposed computational scheme. In Example 1, the objective is to examine the spatiotemporal behavior of the numerical solution and to verify the convergence and stability properties of the method under various parameter settings. In Example 3, the performance of the proposed finite difference scheme given by (28) is compared with the numerical approach reported in [14], allowing for both quantitative and qualitative analysis in terms of accuracy and computational cost. All simulations were implemented in `MATLAB R2022a`. The numerical computations were performed on an `Asus K53SC` laptop equipped with an `Intel Core i5-2430M` processor and `8 GB RAM`. The obtained numerical results demonstrate that the proposed method yields highly accurate and stable solutions while maintaining computational efficiency even on a mid-range hardware platform.

Example 1. Consider the following time-fractional equation:

$$
{}_0^C D_\rho^\alpha \xi(\chi, \rho) = \xi_{\chi\chi} + \mathcal{F}(\xi(\chi, \rho)) + \mathcal{G}(\xi(\chi, \rho)), \quad 0 \leq \rho \leq P, \quad \chi \in \mathbb{R},
$$

where the nonlinear term is considered as follows:

$$\mathcal{F}(\xi) = \xi^2.$$

The source term is obtained in the following form:

$$\mathcal{G}(\chi, \rho) = \frac{e^{-\chi^2} 6\rho^{3-\alpha}}{\Gamma(4-\alpha)} - e^{-\chi^2}(\rho^3 + 1)(4\chi^2 - 2) - e^{-2\chi^2}(\rho^3 + 1)^2.$$

This problem also has the initial condition:

$$\xi(\chi, 0) = e^{-\chi^2},$$

and the exact solution is

$$\xi(\chi, \rho) = e^{-\chi^2}(\rho^3 + 1).$$

In this example, the temporal and spatial discretizations are specified by setting the number of temporal grid points to $N = 320$ and the number of spatial grid points to $M = 2^9$. The fractional order is considered for two representative cases, $\alpha \in \{0.37, 0.68\}$. The spatial step size is given by $h = 1/M$, while the temporal step sizes are chosen as $\varrho \in \left\{\frac{1}{10}, \frac{1}{20}, \frac{1}{40}, \frac{1}{80}, \frac{1}{160}, \frac{1}{320}\right\}$. The spatial computational domain is defined as $I = [a, b] = [-2, 2]$, and the final time is taken as $P = 1$. This example is designed to assess the numerical accuracy of the proposed method for solving time-fractional differential equations with prescribed initial conditions and known analytical solutions. Both numerical and graphical results are provided to illustrate the spatiotemporal behavior of the computed solution and to compare it with the exact analytical solution. The numerical error is defined as follows:

$$E(h, \varrho) = \|e_h^k\|_\infty = \|U_h^k - \xi(\chi_h, \rho_k)\|.$$

The convergence order for the temporal and spatial variations is calculated as follows:

$$\text{order}_1 = \log_2 \frac{E(h, \varrho)}{E(h, \varrho/2)}, \quad \text{order}_2 = \log_2 \frac{E(h, \varrho)}{E(h/2, \varrho)}.$$

Using a fixed spatial step size of $h = 2^{-9}$ and based on the numerical results summarized in Table 1, it is evident that the absolute error $\|e_h^k\|_\infty$ decreases monotonically as the temporal step size ϱ is refined from $\frac{1}{10}$ to $\frac{1}{320}$. This consistent reduction in error confirms the temporal convergence of the proposed scheme. Furthermore, the observed convergence rates, denoted by order_1, for both fractional orders $\alpha = 0.37$ and $\alpha = 0.68$ remain approximately second order, with values ranging between 2.00 and 2.42. The slight reduction of the observed rates compared to the theoretical convergence rate $O(\varrho^{3-\alpha})$ is attributed to the boundary approximations, which slightly limit the global convergence. Nevertheless, the method achieves the expected high-order accuracy at interior points. In particular, the obtained convergence orders slightly exceed those of the classical $L1$ scheme, thereby validating the improved temporal discretization strategy developed in this study. Additionally, the CPU time reported in the last column of Table 1 shows a gradual and proportional increase as the temporal step size decreases. This trend indicates that the computational cost grows moderately with increasing accuracy, confirming the overall efficiency and robustness of the implemented algorithm. Referring to Table 2, the spatial

Table 1: Error results and temporal convergence rates for Example 1 corresponding to various values of α and ϱ.

α	τ	$\|e_h^k\|_\infty$	$order_1$	CPU
0.37	1/10	3.622383e-2	–	0.15
	1/20	9.036367e-3	2.0031	0.27
	1/40	2.098646e-3	2.1063	0.40
	1/80	4.456779e-4	2.2354	0.54
	1/160	8.283166e-5	2.4277	0.85
	1/320	1.783819e-5	2.2152	1.45
0.68	1/10	3.634468e-2	–	0.14
	1/20	9.077627e-3	2.0014	0.21
	1/40	2.129381e-3	2.0919	0.29
	1/80	4.610580e-4	2.2074	0.56
	1/160	9.052296e-5	2.3486	0.83
	1/320	2.168393e-5	2.0617	1.46

convergence behavior of the proposed scheme is analyzed by fixing the temporal step size at $\varrho = 2^{-9}$. It is clearly observed that the absolute error $\|e_h^k\|_\infty$ decreases consistently as the spatial mesh is refined, with h reduced from 1/10 to 1/320. For both fractional orders $\alpha = 0.37$ and $\alpha = 0.68$, the convergence rate, denoted as order_2, remains remarkably stable and very close to the theoretical second-order accuracy, with reported values around 1.99 across all grid refinements. This uniform convergence confirms that the spatial discretization employed in the scheme achieves the expected second-order accuracy, in agreement with the central-difference approximation used for the second spatial derivative. The obtained numerical results demonstrate that the proposed method maintains high spatial accuracy while preserving stability and efficiency. Furthermore, the CPU time values shown in the last column of Table 2 indicate a moderate and proportional increase in computational cost as the grid is refined, confirming the scalability and computational efficiency of the implemented algorithm. In Figure 1, the numerical solution obtained by the present method, (28), is compared with the exact analytical solution for Example 1. The visual comparison reveals excellent agreement between the numerical and exact solutions throughout the entire spatiotemporal domain. This strong consistency verifies the robustness and accuracy of the proposed numerical scheme in capturing the dynamic behavior of the underlying time-fractional problem, both in the temporal and spatial dimensions. The plot

Table 2: Error results and spatial convergence rates for Example 1 corresponding to various values of α and h.

α	h	$\Vert e_h^k \Vert_\infty$	$order_2$	CPU
0.37	1/10	6.804864e-2	–	0.19
	1/20	1.765156e-2	1.9468	0.21
	1/40	4.443487e-3	1.9900	0.32
	1/80	1.112211e-3	1.9983	0.46
	1/160	2.781080e-4	1.9997	0.81
	1/320	6.952907e-5	2.0000	1.43
0.68	1/10	7.850191e-2	–	0.14
	1/20	2.075293e-2	1.9194	0.16
	1/40	5.231265e-3	1.9881	0.30
	1/80	1.309223e-3	1.9984	0.45
	1/160	3.273427e-4	1.9998	0.83
	1/320	8.183599e-5	2.0000	1.46

presented in Figure 2 illustrates the comparison between the numerical and analytical solutions when the spatial step size is fixed at $h = 2^{-9}$ and the temporal step size ϱ is successively refined. It is clearly observed that, as ϱ decreases, the numerical solution progressively approaches the exact analytical solution across the entire computational domain. This uniform improvement in accuracy demonstrates the temporal convergence of the proposed scheme, (28), confirming its numerical consistency with the theoretical prediction based on the Caputo fractional derivative formulation. The close visual agreement between the numerical and exact solutions further verifies the reliability and precision of the method in capturing the transient dynamics of the time-fractional model. The graphical results displayed in Figures 3 and 4 provide a clear and

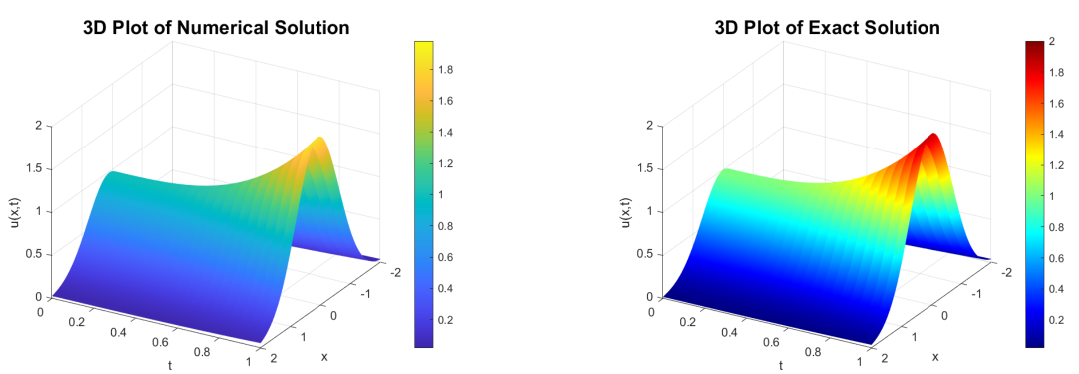

Figure 1: Comparison between the exact solution and the numerical solution of Example 1.

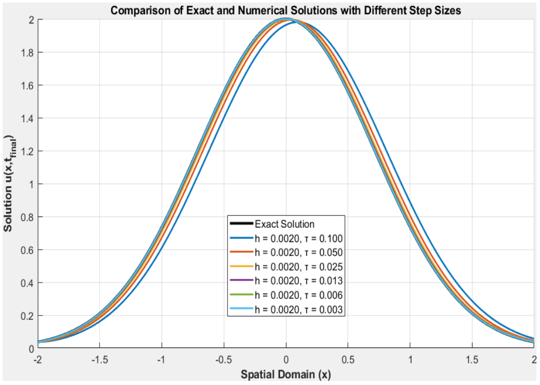

Figure 2: Convergence of the numerical approximation to the exact solution for Example 1.

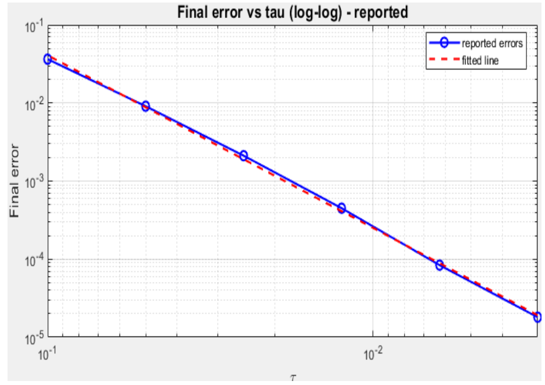

Figure 3: Logarithmic error plot versus ϱ for Example 1.

convincing verification of the theoretical temporal accuracy and stability of the proposed numerical scheme (28). As shown in Figure 3, the log-log representation of the maximum absolute error $\|e_h^k\|_\infty$ versus the time-step size ϱ exhibits an almost perfectly linear decay. The slope of the fitted line corresponds to an observed convergence rate of approximately $p \approx 2.45$, which agrees very well with the theoretical prediction $\mathcal{O}(\varrho^{3-\alpha})$ for $\alpha = 0.37$. This strong agreement between the numerical and theoretical rates confirms that the proposed temporal discretization accurately captures the high-order behavior expected from the fractional derivative formulation. Moreover, the excellent linearity of the data points in the logarithmic scale indicates that the error decreases uniformly with time-step refinement, providing strong evidence of asymptotic temporal consistency and robustness of the scheme. Figure 4 further illustrates the evolution of the absolute error with respect to time for different temporal step sizes. It is clearly observed that as ϱ becomes smaller, the magnitude of the error significantly decreases, and its temporal profile remains smooth and stable throughout the entire simulation period. For sufficiently fine time steps, the error remains nearly constant, indicating that the proposed scheme effectively suppresses error propagation and prevents numerical oscillations. Only for coarser grids does a slight increase in the error magnitude appear near the final time, which is expected due to the accumulation of local truncation errors inherent to fractional-order models. Overall, the results shown in Figures 3 and 4 demonstrate that the proposed method achieves excellent agreement with the theoretical convergence rate, while maintaining remarkable numerical stability even over long-time integrations. These findings confirm the efficiency and reliability of the developed high-order scheme for accurately resolving the transient dynamics of time-fractional nonlinear parabolic equations on unbounded domains. The consistent convergence behavior, combined with the absence of numerical instabilities, strongly validates both the mathematical formulation and the computational implementation of the proposed approach.

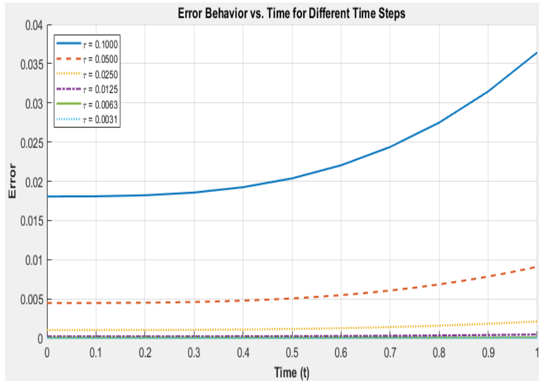

Figure 4: Error behavior for various ϱ values confirming the convergence of the numerical method (28) in Example 1.

Summary: The numerical results presented in Tables 1–2 and Figures 2–4 confirm the high accuracy, stability, and efficiency of the proposed numerical scheme (28). The method exhibits a monotonic decrease in error with both temporal and spatial refinements, achieving convergence rates close to the theoretical orders, $O(\varrho^{3-\alpha})$ in time and $O(h^2)$ in space. Excellent agreement between numerical and analytical solutions validates the correctness of the temporal and spatial discretizations, while the smooth and bounded error evolution confirms unconditional stability. CPU time analysis indicates that computational cost grows moderately with mesh refinement, maintaining a favorable balance between accuracy and efficiency. Overall, the results demonstrate that the proposed approach provides a robust, accurate, and computationally efficient framework for solving time-fractional nonlinear parabolic problems on unbounded domains, effectively fulfilling its theoretical design objectives across all tested configurations. The following Example 2 is introduced to further demonstrate the applicability of the proposed numerical method to physically meaningful problems. Unlike Example 1, which is primarily designed to verify the theoretical convergence behavior of the scheme, the present example considers a nonzero initial condition and a smooth polynomial temporal evolution that commonly arises in diffusion and heat transfer processes with memory effects. The exact solution is chosen as $\xi(\chi,\rho) = e^{-\chi^2}(1+\rho)^3$ which allows the Caputo fractional derivative to be evaluated explicitly without involving special functions such as the Mittag-Leffler function. This choice ensures that the source term can be constructed exactly while preserving analytical simplicity and numerical stability. From a numerical standpoint, this example provides a more comprehensive test of the proposed higher order discretization and absorbing boundary treatment, as it simultaneously incorporates nonlinear effects, fractional temporal memory, and nonzero initial data. Hence, it offers a realistic and robust validation of the effectiveness and accuracy of the proposed method.

Example 2. Consider the following nonlinear time–fractional diffusion equation posed on an unbounded spatial domain:

$$ {}_0^C D_\rho^\alpha \xi(\chi,\rho) = \xi_{\chi\chi} + \mathcal{F}(\xi(\chi,\rho)) + \mathcal{G}(\chi,\rho), \quad 0<\alpha<1, \quad 0\le\rho\le P, \quad \chi\in\mathbb{R}, $$

where the nonlinear reaction term is defined as

$$ \mathcal{F}(\xi) = \xi^2 + \xi. $$

The initial condition is given by

$$ \xi(\chi,0) = e^{-\chi^2}. $$

We choose the exact solution in the form

$$ \xi(\chi,\rho) = e^{-\chi^2}(1+\rho)^3, $$

the source term is constructed as

$$ \begin{aligned} \mathcal{G}(\chi,\rho) = e^{-\chi^2}&\left[\frac{4!}{\Gamma(4-\alpha)}\rho^{3-\alpha} + 3\frac{3!}{\Gamma(3-\alpha)}\rho^{2-\alpha} + 3\frac{2!}{\Gamma(2-\alpha)}\rho^{1-\alpha}\right] \\ &- (4\chi^2-2)e^{-\chi^2}(1+\rho)^3 - e^{-2\chi^2}(1+\rho)^6. \end{aligned} $$

Table 3: Temporal convergence results for Example 2 with $h = 1/2^9$.

α	τ	$\|e_h^k\|_\infty$	$order_1$	CPU
0.37	1/10	1.471500e-1	–	0.28
	1/20	3.662159e-2	2.0065	0.35
	1/40	8.584786e-3	2.0928	0.47
	1/80	1.864492e-3	2.2029	0.84
	1/160	3.687139e-4	2.3382	1.13
	1/320	8.914893e-5	2.0482	1.97
0.68	1/10	1.474604e-1	–	0.17
	1/20	3.677890e-2	2.0033	0.28
	1/40	8.663713e-3	2.0858	0.41
	1/80	1.903987e-3	2.1859	0.72
	1/160	3.884649e-4	2.2931	1.17
	1/320	9.102469e-5	2.0934	2.00

Example 3. Consider the following problem:

$$ {}_0^C D_\rho^\alpha \xi(\chi,\rho) = \xi_{\chi\chi} + \mathcal{F}(\xi) \quad \chi\in\mathbb{R}, \quad 0<\rho\le P, $$

with the initial condition given by

Table 4: Spatial convergence results for Example 2 with $\tau = 1/2^9$.

α	h	$\|e_h^k\|_\infty$	$order_2$	CPU
0.37	1/10	3.270424e-1	–	0.15
	1/20	8.452788e-2	1.9519	0.27
	1/40	2.124029e-2	1.9926	0.45
	1/80	5.313965e-3	1.9989	0.67
	1/160	1.328601e-3	1.9998	1.08
	1/320	3.321506e-4	1.9999	2.05
0.68	1/10	3.510207e-1	–	0.13
	1/20	9.244171e-2	1.9249	0.24
	1/40	2.326518e-2	1.9903	0.40
	1/80	5.820151e-3	1.9990	0.65
	1/160	1.455053e-3	1.9999	1.15
	1/320	3.637556e-4	2.0000	2.07

$$\xi(\chi, 0) = \left(\frac{1}{1 + e^{-\frac{6\chi}{4}}}\right)^{\frac{1}{3}},$$

and the exact solution defined as

$$\xi(\chi, \rho) = \left(\frac{1}{1 + e^{-\frac{15\rho+6\chi}{4}}}\right)^{\frac{1}{3}},$$

The nonlinear function $\mathcal{F}(\xi)$ is defined by

$$\mathcal{F}(\xi) = \xi(1 - \xi^6),$$

The numerical method employed in [14] to solve the above problem is described as follows:

$$\begin{aligned}
&{}_0^C D_\rho^\alpha \xi_i^k = \sigma_\chi^2 \xi_i^k + \mathcal{F}(\xi_i^{k-1}), \quad 1 \le k \le N, \quad 1 \le i \le M-1,\\
&\sigma_\chi \xi_1^k = \Phi_k + 3s_0^{\alpha/2}\xi_0^k + \frac{h}{2}\left({}_0^C D_\rho^\alpha \xi_0^k - \mathcal{F}(\xi_0^{k-1})\right),\\
&\sigma_\chi \xi_{M-1}^k = \Psi_k - 3s_0^{\alpha/2}\xi_M^k - \frac{h}{2}\left({}_0^C D_\rho^\alpha \xi_M^k - \mathcal{F}(\xi_M^{k-1})\right),\\
&{}_0^C D_\rho^\alpha \Phi_k = \left(\mathcal{F}(\xi_0^{k-1}) - 3s_0^\alpha\right)\Phi_k + \left(8s_0^{3\alpha/2} - 3s_0^{\alpha/2}\mathcal{F}(\xi_0^{k-1})\right)\xi_0^k + 3s_0^{\alpha/2}\mathcal{F}(\xi_0^{k-1}),\\
&{}_0^C D_\rho^\alpha \Psi_k = \left(\mathcal{F}(\xi_M^{k-1}) - 3s_0^\alpha\right)\Psi_k - \left(8s_0^{3\alpha/2} - 3s_0^{\alpha/2}\mathcal{F}(\xi_M^{k-1})\right)\xi_M^k - 3s_0^{\alpha/2}\mathcal{F}(\xi_M^{k-1}),\\
&\xi_i^0 = \xi_0(\chi_i), \quad \Phi_0 = \varphi(0), \quad \Psi_0 = \phi(0).
\end{aligned} \tag{63}$$

Table 5 presents the maximum errors $\|e_h^k\|_\infty$ at the final time P for different time step sizes ϱ and fractional orders α, with a fixed spatial step size $h = 2^{-8}$. The results indicate that the proposed method achieves significantly higher temporal accuracy compared to the method in

[14], with a convergence rate (Order1) between 2.31 and 2.63, consistent with the theoretical order $O(\varrho^{3-\alpha} + h^2)$. In contrast, the method of [14] has a theoretical temporal accuracy of $O(\varrho + h^2)$, which explains why the observed convergence rate in time (Order1) is limited to approximately 0.98–1.00. As the time step ϱ decreases from 1/10 to 1/160, the maximum error of the proposed method drops sharply; for example, with $\alpha = 0.37$, the error decreases from 5.71×10^{-2} to 3.88×10^{-5}, while the corresponding error for the method in [14] reduces only from 2.47×10^{-2} to 1.60×10^{-3}. This demonstrates a significantly faster convergence of the proposed method to the exact solution. Increasing the fractional order from $\alpha = 0.37$ to $\alpha = 0.68$ slightly reduces the temporal convergence rate, as predicted by the term $(3-\alpha)$ in the theoretical order, but the proposed method consistently outperforms the reference method for all α, maintaining lower error values and stable behavior. The smooth, monotonic decrease of errors with decreasing ϱ confirms the robust numerical stability of the proposed scheme, with no oscillations or divergence observed even for very fine temporal grids. Overall, these results indicate that the proposed method achieves both higher temporal accuracy and faster convergence than the method in [14], and its superior performance is especially pronounced on finer temporal grids, highlighting its suitability for applications where temporal precision is critical. The observed

Table 5: Temporal errors and convergence of the proposed method for Example 3.

α	ϱ	Our method (28)	order1	Method in [14]	order1
0.37	1/10	$5.7138196e-2$	–	$2.465416e-2$	–
	1/20	$9.2080193e-3$	2.6334	$1.246783e-2$	0.98
	1/40	$1.4874461e-3$	2.6300	$6.285612e-3$	0.99
	1/80	$2.4005411e-4$	2.6314	$3.170451e-3$	0.99
	1/160	$3.8839013e-5$	2.6277	$1.595221e-3$	0.99
0.68	1/10	$3.1182567e-2$	–	$3.945612e-2$	–
	1/20	$6.2297534e-3$	2.3234	$1.985421e-2$	0.99
	1/40	$1.2475707e-3$	2.3200	$9.963412e-3$	0.99
	1/80	$2.4960448e-4$	2.3214	$4.993210e-3$	0.99
	1/160	$5.0064596e-5$	2.3177	$2.500843e-3$	1.00

differences in temporal convergence rates between Examples 1 and 3 are expected due to the distinct problem setups. In Example 1, a small spatial domain $[-2, 2]$ with a nonzero source term was considered, whereas Example 3 involves a larger domain $[-20, 20]$ under homogeneous conditions ($\mathcal{G}(\chi, \rho) = 0$). The larger computational domain in Example 3 allows for smoother spatial variations, reducing the relative impact of spatial discretization on the overall error and enabling the temporal convergence to closely approach the theoretical order. Conversely, in Example 1, the presence of the source term and the smaller domain induces steeper gradients and localized dynamics, which slightly diminish the observed temporal convergence rate. Moreover, the homogeneous nature of Example 3 promotes uniform and stable numerical behavior, allowing the method to achieve higher temporal accuracy ($Order1$ between 2.32 and 2.63) compared to Example 1 ($Order1$ between 2.0 and 2.42). Therefore, these differences reflect the natural influence of domain size, source term, and boundary conditions, rather than any deficiency in the numerical scheme. Figures 5 and 6 present the two-dimensional and three-dimensional plots of the numerical solution obtained by applying the method introduced in (28) to the problem described in Example 3. The results demonstrate a clear convergence of the numerical solution to the analytical solution, exhibiting excellent agreement in both spatial and temporal dimensions. These plots confirm that the proposed numerical scheme performs consistently with the theoretical predictions regarding accuracy, stability, and convergence. The visual evidence, combined with the quantitative analysis presented in Table 5, reinforces the reliability and robustness of the method for capturing the solution behavior with high fidelity across the computational domain.

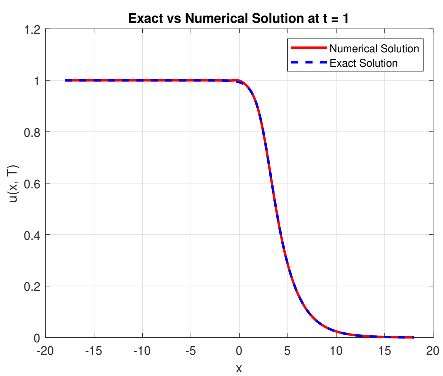

Figure 5: Convergence behavior of the numerical solution toward the exact solution for Example 3.

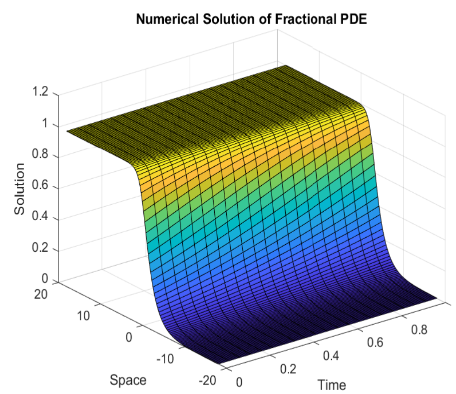

Figure 6: Numerical solution plot for Example 3.

6 Conclusions

This study presents a novel, rigorously analyzed, and computationally efficient framework for the numerical solution of nonhomogeneous time-fractional nonlinear parabolic equations defined on unbounded spatial domains. The core challenges of temporal nonlocality, inherent nonlinearity, and the infinite spatial extent were addressed through a fundamentally new approach. The methodology's cornerstone is the derivation of highly accurate ABCs, constructed directly from the fundamental properties of fractional derivatives. This principled approach circumvents the limitations of existing techniques based on Padé approximations, ensuring a faithful representation of the underlying fractional dynamics at domain boundaries. By effectively truncating the infinite domain to a finite computational region while minimizing spurious reflections, these ABCs transform the original intractable problem into an equivalent, well-posed formulation on a bounded domain. The resulting bounded domain problem was discretized using a high-order finite difference scheme, facilitating stable and precise numerical implementation. A comprehensive theoretical analysis established the unconditional stability of the proposed method and provided rigorous error bounds, guaranteeing the reliability of the obtained solutions. Extensive numerical experiments unequivocally demonstrate the practical efficacy and robustness of the framework. The method achieves high accuracy in capturing the complex, memory-dependent behaviors characteristic of fractional-order systems, even in the presence of strong nonlinearities. Numerical results further confirm the superior accuracy and stability of the proposed method compared to existing approaches for unbounded domains, while maintaining a significantly reduced computational burden. Consequently, this work provides a powerful, reliable, and efficient computational tool for simulating anomalous diffusion and related complex phenomena governed by time-fractional dynamics in unbounded settings. The framework has direct relevance to diverse applications across physics, biology, and engineering. Moreover, it lays a solid foundation for future extensions to multi-dimensional scenarios, stochastic fractional PDEs, and problems involving variable coefficients, highlighting the potential for further development and application in complex fractional systems.

Future directions

Building upon the results of this study, several promising research directions can be explored. The proposed numerical framework can be extended to multi-dimensional time-fractional nonlinear parabolic equations defined on unbounded domains. Another important direction is the generalization of the ABCs to space-fractional and distributed-order models. Furthermore, the development of adaptive time-stepping and spatial refinement strategies could significantly improve computational efficiency for long-time simulations. Extending the present high-order scheme to coupled systems, stochastic FPDEs, and problems with variable coefficients also represents a meaningful avenue for future research. Finally, applying the proposed method to real-world models arising in physics, biology, and engineering may further demonstrate its practical relevance and versatility.

Author declaration

The authors have no conflicts to disclose.

Funding

This research received no external funding.

Conflicts of Interest

The authors declare no conflicts of interest.

References

[1] Agrawal, O.P. *A general solution for the fourth-order fractional diffusion-wave equation*, Fract. Calc. Appl. Anal. 3(1) (2000), 1–12.

[2] Akrami, M.H., Poya, A. and Zirak, M.A. *Solving the general form of the fractional Black–Scholes with two assets through reconstruction variational iteration method*, Results. Appl. Math. 22 (2024), 100444.

[3] Cao, J., Li, C. and Chen, Y. *High-order approximation to Caputo derivatives and Caputo-type advection-diffusion equations (II)*, Fract. Calc. Appl. Anal. 18 (2015), 735–761.

[4] Engquist, B. and Majda, A. *Absorbing boundary conditions for the numerical simulation of waves*, Math. Comput. 31(139) (1977), 629–651.

[5] Gao, G., Sun, H. and Sun, Z.Z. *The finite difference approximation for a class of fractional sub-diffusion equations on a space unbounded domain*, J. Comput. Phys. 236 (2013), 443–460.

[6] Gao, G., Sun, H. and Zhang, Y.N. *A finite difference scheme for fractional sub-diffusion equations on an unbounded domain using artificial boundary conditions*, J. Comput. Phys. 231(7) (2012), 2865–2879.

[7] Gao, G.H., Sun, Z.Z. and Zhang, H.W. *A new fractional numerical differentiation formula to approximate the Caputo fractional derivative and its applications*, J. Comput. Phys. 259 (2014), 33–50.

[8] Han, H. and Huang, Z. *A class of artificial boundary conditions for heat equation in unbounded domains*, Comput. Math. Appl. 43(6-7) (2002), 889–900.

[9] Han, H., Sun, Z.Z. and Wu, X.N. *Convergence of a difference scheme for the heat equation in a long strip by artificial boundary conditions*, Numer. Methods Partial Differ. Equ. 24(1) (2008), 272–295.

[10] Hashemi, M.S., Mirzazadeh, M., Bayram, M. and El Din, S.M. *Numerical approximation of the Cauchy non-homogeneous time-fractional diffusion-wave equation with Caputo derivative using shifted Chebyshev polynomials*, Alex. Eng. J. 81 (2023), 118–129.

[11] Jiang, S., Zhang, J., Zhang, Q. and Zhang, Z. *Fast evaluation of the Caputo fractional derivative and its applications to fractional diffusion equations*, Commun. Comput. Phys. 21(3) (2017), 650–678.

[12] Kilbas, A.A. and Srivastava, H. M. and Trujillo, J. J. *Theory and applications of fractional differential equations*, Elsevier 204, 2006.

[13] Li, C., Wang, R., Du, H. and Pagnini, G. *High-order approximation to Caputo derivatives and Caputo-type advection-diffusion equations*, Commun. Appl. Ind. Math. 299 (2015), 159–175.

[14] Li, D. and Zhang, J. *Efficient implementation to numerically solve the nonlinear time fractional parabolic problems on unbounded spatial domain*, J. Comput. Phys. 322 (2016), 415–428.

[15] Magin, R. *Fractional calculus in bioengineering, part 1*, Crit. Rev. Biomed. Engin. 32(1) (2004), 1–34.

[16] Metzler, R. and Klafter, J. *Boundary value problems for fractional diffusion equations*, Phys. A: Stat. Mech. Appl. 278(1-2) (2000), 107–125.

[17] Nikan, O., Rashidinia, J. and Jafari, H. *Numerically pricing American and European options using a time fractional Black–Scholes model in financial decision-making*, Alex. Eng. J. 112 (2025), 235–245.

[18] Podlubny, I. *Fractional differential equations: An introduction to fractional derivatives, fractional differential equations, to methods of their solution and some of their applications*, Elsevier, 198, 1998.

[19] Povstenko, Y. *Signaling problem for time-fractional diffusion-wave equation in a half-plane*, Fract. Calc. Appl. Anal. 11(3) (2008), 331–349.

[20] Povstenko, Y. *Signaling problem for time-fractional diffusion-wave equation in a half-space in the case of angular symmetry*, Nonlinear Dyn. 59 (2010), 593–605.

[21] Schneider, W.R. and Wyss, W. *Fractional diffusion and wave equations*, J. Math. Phys. 30(1) (1989), 134–144.

[22] Senfiazad, P., Heydari, M.H., Bayram, M. and Baleanu, D. *A numerical method based on the shifted Jacobi polynomials for a class of tempered fractional quadratic integro-differential equations*, Results Appl. Math. 27 (2025), 100601.

[23] Sun, Z. Z. and Wu, X. *A fully discrete difference scheme for a diffusion-wave system*, Appl. Numer.Math. 56(2) (2006), 193–209.

[24] Wang, F., Ahmad, I., Ahmad, H., Alsulami, M.D., Alimgeer, K.S., Cesarano, C. and Nofal, T. A. *Meshless method based on RBFs for solving three-dimensional multi-term time fractional PDEs arising in engineering phenomenons*, J. King Saud Univ. Sci. 33(8) (2021), 101604.

[25] Wang, F., Khan, M.N., Ahmad, I., Ahmad, H., Abu-Zinadah, H. and Chu, Y.M. *Numerical solution of traveling waves in chemical kinetics: time-fractional fishers equations*, Fract. 30(02) (2022), 2240051.

[26] Wyss, W. *The fractional diffusion equation*, J. Math. Phys. 27(11) (1986), 2782–2785.

[27] Zhuang, P. and Liu, F. *Implicit difference approximation for the time fractional diffusion equation*, J. Appl. Math. Comput. 22 (2006), 87–99.